

**Study on the Treatment for Large Bone Defects  
with Basic Fibroblast Growth Factor-  
incorporated Tailor-made Artificial Bones in Dogs**  
(犬の大きな骨欠損に対する塩基性線維芽細胞増殖因子  
結合テーラーメイド人工骨による  
治療法に関する研究)

崔 成 眞

**Study on the Treatment for Large Bone Defects  
with Basic Fibroblast Growth Factor-  
incorporated Tailor-made Artificial Bones in Dogs**  
(犬の大きな骨欠損に対する塩基性線維芽細胞増殖因子  
結合テーラーメイド人工骨による  
治療法に関する研究)

**Laboratory of Veterinary Surgery  
Department of Veterinary Medical science  
Graduate School of Agricultural and Life Sciences  
The University of Tokyo**

東京大学大学院農学生命科学研究科  
獣医専攻博士課程 獣医外科学研究室

平成18年度入学

**Sungjin CHOI**

崔 成 眞

# CONTENTS

<b>General Introduction .....</b>	<b>1</b>
Bone grafts .....	2
Artificial bones .....	3
Tailor-made artificial bones .....	5
Fibroblast Growth Factor as an osteoinductive factor .....	6
Purpose of this study .....	8
<b>Chapter 1. Fabrication of bFGF-incorporated tailor-made artificial implant with trehalose-coating .....</b>	<b>10</b>
Introduction .....	11
Materials & Methods .....	14
Results .....	19
Discussion .....	22
<b>Chapter 2. Bone regeneration by implantation of bFGF-incorporated tailor-made implants with trehalose coating on the defect of the skull in dogs .....</b>	<b>33</b>
Introduction .....	34
Materials & Methods .....	36
Results .....	42
Discussion .....	45

**Chapter 3. Long-term effectiveness of trehalose-coated and bFGF-incorporated implants for critical size defect of the skull of dogs..... 59**

Introduction..... 60

Materials & Methods..... 62

Results..... 69

Discussion..... 74

**Chapter 4. Effect of implantation of bFGF-incorporated tailor-made implants on the repair of radial segmental defects in dogs94**

Introduction..... 95

Materials & Methods..... 98

Results..... 103

Discussion..... 105

**Conclusion.....116**

**Acknowledgment..... 120**

**References..... 121**

# **General Introduction**

## **Bone grafts**

Bone graft is often essential to repair large bone defects caused by the congenital deformity, bone injury and skeletal tumor removal. An ideal bone graft substitute should have functions to provide (1) osteoconductive matrix that acts as a scaffold for new bone ingrowth, (2) osteoinductive factors that induce the differentiation of osteoblastic cells from undifferentiated osteoprogenitor cells and (3) osteogenic cells that produce new bone formation.

Bone grafts can be divided into three main categories based on where they are obtained.

Autograft is the bone tissue usually harvested from patient's iliac crest or humeral head. It is considered to be the "gold standard" to repair bone defects because they are rich in cancellous bones containing many osteoinductive factors and osteoblasts. However, it also has problems such as surgical invasion at the donor site, limited sources of bones and possibility of seroma, hematoma, postoperative pain at the harvesting site (Arrington *et al.* 1996; Sen *et al.* 2007).

Allograft is the bone tissue harvested from other individuals of the same species. Allograft bone is principally osteoconductive, although it may have some osteoinductive capability, depending on how it is processed (Stevenson 1999). However,

it can induce the infection or immunologic reaction in the recipient (Stevenson *et al.* 1996; Mankin *et al.* 2005).

Xenograft is the bone tissue harvested from other species. Xenograft would be available from unlimited sources. However, the extreme histocompatibility mismatch between human recipients and xenograft bone materials caused the severe limiting factors to use this approach in the clinical practice (Levai *et al.* 2003). To resolve these problems, the alternative material should be required.

### **Artificial bones**

Since the first report on the artificial bone in 1940s (Schram *et al.* 1948), the various type of artificial bones have been developing as an alternative to bone grafts. The artificial bone substitute materials are made from metals, ceramics, polymers, and others (Ratner *et al.* 2004). Nowadays, calcium phosphate-based materials such as hydroxyapatite and tricalcium phosphate have been used widely in the clinical practice because they have excellent biocompatibility and osteoconductivity than other materials (Trombelli *et al.* 2002; Simpson *et al.* 2004; Nair *et al.* 2009).

Hydroxyapatite has the same structure with calcium phosphate as bone minerals. It can be used as various types of materials; dense or porous structure and granules or

blocks. Some hydroxyapatites are sintered to possess pertinent mechanical strength. Its mechanical strength was various depending on the manufacturing procedures (He *et al.* 2008). However, sintered hydroxyapatite has little plasticity and takes a longer period to be displaced by new bones in *in vivo* condition (Goto *et al.* 2001).

Tricalcium phosphates (TCP) is subdivided into alpha and beta form by its crystallinity. Alpha-tricalcium phosphate ( $\alpha$ -TCP)-oriented artificial bone has been used in the paste form which is composed of powder mixture and liquid component. It has good mechanical strength and manipulability, and can be infused into the small hole during surgery (Ikeuchi *et al.* 2001; Takemasa *et al.* 2002). However, it needs long time for hardening at the graft site and is difficult to apply for the bone defect with complicated shapes (Komuro 2003; Baba *et al.* 2008).

Beta-tricalcium phosphate ( $\beta$ -TCP)-oriented artificial bone has been used in the porous block or granular form and showed excellent biodegradability. However, despite of its good biodegradability, it is generally fragile and easily brittle. The replacement of  $\beta$ -TCP by recipient's new bone does not occur in an equitable way (Hollinger *et al.* 1996; Moore *et al.* 2001).

## **Tailor-made artificial bones**

The increasing technology of computer-based three-dimensional (3D) imaging procedures in the field of medicine and engineering has contributed the potential of rapid prototyping (RP) techniques. RP is the automatic construction of physical objects using additive manufacturing technology. The first techniques for RP became available in the late 1980s and were used to produce models and prototype parts. Today, they are used for a much wider range of applications such as medical and biomedical sectors (Curodeau *et al.* 2000; Webb 2000). There are several RP machines, selective laser sintering (SLS), fused deposition modeling (FDM), stereolithography (STL), laminated object manufacturing (LOM), electron beam melting (EBM) and 3D printing (3DP). Each has their characteristics (Sun *et al.* 2004).

Tailor-made artificial bones made of  $\alpha$ -TCP fabricated using a 3D ink-jet printer by 3DP techniques has been developed (Igawa *et al.* 2006). For fabrication, the CT data were first obtained from patient's bone defect area. The obtained CT data were converted to computer-aided design (CAD) data using STL program. Based on the 3D image, the artificial bone was fabricated from a 3D ink-jet printer (Fig. 0-1).

Because tailor-made artificial bones were fabricated based on CT data of the bone defect, they were well matched to the shape of the bone defect and could be easily

implanted to the defect site. In addition, it can freely design the internal structure of the implant to create the cylindrical hole which can facilitate bone ingrowth (Igawa *et al.* 2006). However, the tailor-made artificial bones up to the present have only osteoconductivity, not osteoinductivity.

### **Fibroblast Growth Factor as an osteoinductive factor**

Osteoinductive factors have the function to differentiate osteogenic cells into osteoblasts or proliferate osteogenic cells through their own signal pathways. Various osteoinductive factors have been identified up to date, including bone morphogenetic protein (BMP), fibroblast growth factor (FGF), insulin-like growth factor (IGF), transforming growth factor beta (TGF- $\beta$ ) and platelet derived growth factor (PDGF) (Lieberman *et al.* 2002). FGF is a family of polypeptides and controls the proliferation and differentiation of various cell types depending on the cell maturation (Basilico *et al.* 1992; Jaye *et al.* 1992). FGF superfamily can be currently subdivided into 23 families. Among these, FGF-2 (known as basic FGF; bFGF), FGF 9 and FGF 18 are demonstrated to be expressed on osteoprogenitor cells and have capacity of potent proliferation of osteoblastic cells (Rodan *et al.* 1989; Kawaguchi 2005).

The actions of FGFs are dependent on the spatiotemporal pattern of expression of

high affinity FGF receptors (FGFR) (Givol *et al.* 1992; Powers *et al.* 2000). FGFR1 and FGFR2 are expressed in mesenchymal cells during condensation of mesenchyme prior to deposition of the bone matrix at early stages of long bone development, and are also expressed in the cranial suture (Orr-Urtreger *et al.* 1991; Delezoide *et al.* 1998). Later in the development and in the postnatal life, FGFR1 and FGFR2 are found in pre-osteoblasts and osteoblasts together with FGFR3. And, FGFR4 is also expressed in mouse skull and primary osteoblasts (Cool *et al.* 2002).

bFGF plays important roles in skeletal development (Naski *et al.* 1998) and in fracture repair (Kawaguchi *et al.* 1994; Wildburger *et al.* 1994). bFGF has potent capability to proliferate osteoblastic cells *in vitro* and *in vivo* (Rodan *et al.* 1989; Wang *et al.* 1996). bFGF-disrupted mouse shows decreased bone mass and bone formation (Montero *et al.* 2000).

In *in vivo* studies, systemic injections of bFGF to the animals bone defect enhanced endosteal bone formation (Nagai *et al.* 1995; Nakamura *et al.* 1995). A study showed that bFGF given into a bone defect without a carrier induced significantly less bone ingrowth than with a carrier (Tabata *et al.* 1998). Therefore, adequate scaffolds should be essential to enhance their biological activity. Currently human recombinant bFGF is commercially available in Japan under the approval of Ministry of Health, Labor and

Welfare. Therefore in this thesis, I selected this bFGF as an osteoinductive agent.

## **Purpose of this study**

The purpose of this study was to investigate the clinical applicability of tailor-made artificial bones incorporated with bFGF to repair the large bone defect in dogs.

In Chapter 1, I fabricated the bFGF-incorporated tailor-made artificial bone made from  $\alpha$ -TCP and evaluated its *in vitro* cell proliferative effect, mechanical strength and the surface structure of artificial bone. In Chapter 2, I investigated the bone regenerative effects of this bFGF-incorporated tailor-made artificial bone and the optimal dose of bFGF for using an experimental skull defect model in dogs. In Chapter 3, I investigated the long-term effect of this implant for the defect of the skull with a critical size in dogs. Finally, in Chapter 4, I investigated the potential usefulness of this artificial bone for the defect of the load-bearing site using radial defect model of dogs.

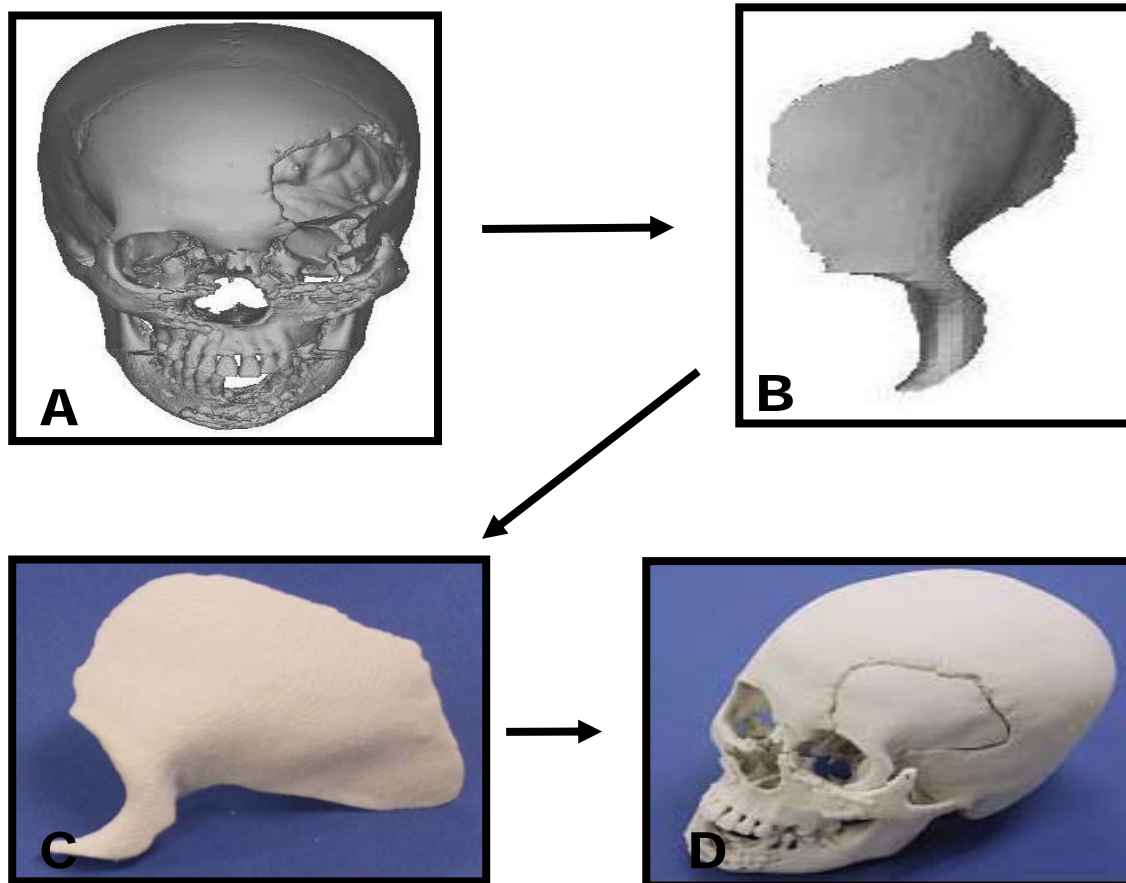


**Fig. 0-1** Fabrication flow of a tailor-made artificial bone. (A) CT scanning for bone defect, (B) CT data were converted to CAD data by STL program, (C) fabricate the artificial bone using 3D inkjet printer, and (D) implant the artificial bone to the defect with the similar shape (Referred from the data of NEXT 21 Co.).

**Chapter 1. Fabrication of bFGF-incorporated tailor-made artificial implant with trehalose-coating**

## Introduction

The artificial bone has an excellent osteoconductive function, but no osteoinductive function. With less osteoinductive function, the stabilization and replacement by regenerative new bones of implanted artificial bone will be delayed after implantation. To solve the problem, a research has been conducted to increase the regenerative capability of the implant by incorporating various osteoinductive factors to them (Hutmacher *et al.* 2007).

The tailor-made implant developed by our group. It was fabricated from  $\alpha$ -TCP using a 3D inkjet printer and showed excellent osteoconductivity (Igawa *et al.* 2006).

Osteoinductive factors such as bone morphogenetic protein (BMP) and basic fibroblast growth factor (bFGF) can differentiate and proliferate the osteoblastic cells (Yamaguchi *et al.* 2000; Wronski 2001; Canalis *et al.* 2003; Kawaguchi 2005). However, they need an adequate carrier to enhance their biological activity. Calcium phosphates has been used as a drug delivery system(DDS) for these osteoinductive factors because of their self-setting ability, injectability and degradability (Ginebra *et al.* 2006; Habraken *et al.* 2007). DDS should incorporate and store the drug molecules and release them at the preferable phase without inactivation of the molecules. Calcium phosphate absorbs the protein strongly than other materials (Talal *et al.* 2009). Binding affinity of

calcium phosphate with these proteins may be too strong to release them (Midy *et al.* 1998). The incorporated proteins sometimes could not be released from calcium phosphate in physiological pH, leading to fail to show their effective function (Matsumoto *et al.* 2004). These reports may suggest that bFGF incorporated to the tailor-made artificial bone made of  $\alpha$ -TCP may not be released at an appropriate time.

In my preliminary experiments *in vitro*, these problems were solved through inhibition of the direct binding of the bFGF to calcium phosphate using serine, dextran and trehalose, then inhibitory function of these agents were almost similar.

Trehalose is a non-reducing disaccharide found in a wide variety of natural organisms. Although the mechanism of the cell-protecting function of trehalose is still unclear, trehalose can protect the integrity of cells against a variety of environmental stresses such as desiccation, dehydration, freezing and oxidation. Trehalose may have protective function of protein molecules of the cells. Through these protective effects of trehalose observed in living systems, trehalose has been widely used in the food, cosmetics and drugs (Richards *et al.* 2002; Elbein *et al.* 2003; Chen *et al.* 2004). Through these wide function of trehalose, coating of the artificial bone may prevent strong incorporation of bFGF by  $\alpha$ -TCP of the artificial bone. Therefore in this study, I selected trehalose to inhibit strong binding of bFGF with artificial bones.

Another problem of the tailor-made artificial bone was fragile especially when it was soaked within the water. When a trehalose solution will be used to coat the artificial bone, the artificial bone may become fragile, which may decrease the value of the artificial bone in clinical practice. Furthermore, detail structure and mechanical strength of the artificial bone with or without trehalose-coating were not yet clarified.

In this chapter, I conducted an *in vitro* study is attempt to confirm whether trehalose could prevent the strong binding of bFGF by the artificial bone and allow to release bFGF from the implant in the adequate phase. In addition, I also measure the microstructure, qualitative analysis and mechanical strength of the artificial bone, and their changes after trehalose coating.

## Materials & Methods

### *Preparation of implants*

**Implant fabrication:** Fabrication of the artificial bone was similar to those described in the previous report (Igawa *et al.* 2006; Choi *et al.* 2009). Briefly, the tailor-made implant (TI) was designed for each experiment based on 3D images of computed tomography (CT) of each dog using the software Mimics program (Materialise, Leuven, Belgium) and fabricated by a 3D ink-jet printer (Z406 3D color printer: Z-corporation, Burlington, USA). The fabrication process is shown in Fig. 1-1. Liquid binder was ejected from the ink jet head to a powder layer with 0.1 mm in thickness to bond the surface of the powder layer into the desired shape. By the function of the liquid binder, hardening of the powder material on the flat surface was obtained and a solid figure was formed. The powder used was  $\alpha$ -TCP (Biopex, Mitusubishi Materials, Tokyo, Japan) with the mean particle diameter being 10 $\mu$ m. The liquid binder was a mixture of 5% sodium chondroitin sulfate (Seikagaku, Tokyo, Japan), 12% disodium succinate (Wako, Tokyo, Japan) and 83% distilled water (Otsuka Pharmaceuticals, Tokyo, Japan). Each hardened sheet was piled repeatedly, then desired shape of the artificial bone was produced.

**Trehalose coating:** Trehalose was purchased from Hayashibara Corporation

(Okayama, Japan). For trehalose coating, implants were immersed in 5% trehalose solution at room temperature for overnight after fabrication. Then, implants were washed with distilled water and autoclaved at 121 °C for 30 minutes. Finally, implants were dried under air pressure.

**bFGF infiltration:** recombinant human-bFGF was purchased from Kaken Pharmaceuticals (Tokyo, Japan) and diluted with deionized water into 1 µg/µl solution. The bFGF solution was dropped with a micropipette to implants with or without trehalose-coating, and dried for 10 minutes at room temperature, immediately before the experiment.

#### *Effect of bFGF incorporated with the artificial bone on cell proliferation in vitro*

Disk-shaped artificial bone implants with 4 mm in diameter and 2 mm in height were prepared for the cell proliferation test. Implants were divided into the following 4 groups of 3 each; implants without trehalose-coating, implants with trehalose-coating alone, bFGF-incorporated implants without trehalose-coating, bFGF-incorporated implants with trehalose-coating.

The *in vitro* experiment was conducted as follows. MC3T3-E1 cells, mouse osteoblastic cells, were used in this study. MC3T3-E1 cells were cultured in the

standard culture medium of Dulbecco's modified Eagle medium (DMEM; Gipro, NY, USA), supplemented with 10% fetal bovine serum (FBS; Gipro), 200 mg/ml penicillin (Gipro), and 200 mg/ml streptomycin (Gipro) at 37 in a humidified atmosphere of 5% CO<sub>2</sub>. The medium was changed every 2 or 3 days. The cells were seeded in a 96-well plate at 5,000 cells/well density and incubated for 24 hours.

Fig. 1-2 shows the schematic figure of the culture method in this experiment. The implants were inserted in the cell inserter. In addition, cell culture without implants and bFGF was performed as a negative control. Also cell culture without implants but with 10 µg bFGF was performed as a positive control. The cells of all groups were incubated for 48 hours, then 10 µl of cell counting kit-8 solution (Dojindo, Kumamoto, Japan) was added to each well of the plate and incubated for another 4 hours. The number of viable cells in the culture medium was measured at the absorbance of 450nm using a microplate reader.

### ***Scanning electron microscope***

The scanning electron microscope (SEM) was used to observe the structure and superficial morphology of the implant with or without trehalose-coating. The implant was lyophilized and observed with SEM (JCM -5700, JEOL, Tokyo, Japan) at an

accelerating voltage of 1.2 kV.

### ***X-ray diffraction (XRD) for qualitative analysis***

An X-ray diffractometer (Miniflex II, Rigaku, Tokyo, Japan) was used to assess the crystallinity of the implant with or without trehalose-coating. The X-ray source was CuK $\alpha$ , and X-ray diffraction was performed at 30 kV and 15 mA with a scanning speed of 2°/min. X-ray diffraction patterns were indexed according to the structural data of powder diffraction file (ICDD).

### ***Mechanical strength***

Implants of two different sizes were prepared. Each implant was soaked in 5% trehalose solution or 0.9% saline for overnight and washed with distilled water and autoclaved at 121 °C for 30 minutes. Implants without these treatments were used as a control. The implant with 7 mm in width and 17 mm in height was used for measurement of mechanical strength, which was evaluated using the compression strength test. The maximum compression load strength was calculated as a following fomula.

$$\text{Maximum compression load strength} = \frac{4N}{(\pi r)^2}$$

(N: load, r: diameter of implant)

Another implant with 40 mm in width and 30 mm in height was used for evaluation of three point bending strength. The maximum three point bending load strength was calculated by formula below.

$$\text{Maximum bending load strength} = \frac{30 \times 3N}{2wh^2}$$

(N: load, w: width of implant, h: height of implant)

Strength test was performed by INSTRON universal testing machine (Instron-3365, Instron Corporation, Norwood, USA) with a load cell of 5kN and load speed at 1.0 mm/min.

### ***Statistical analysis***

For the data on cell proliferation and mechanical strength, the mean and standard deviations (SD) of each group was calculated, and student t-test was performed using spreadsheet program (Excel, Microsoft). P value less than 0.05 was considered statistically significant.

## **Results**

### ***Cell proliferation in vitro***

Fig. 1-3 show the proliferation rate of each group. The number of cells viable of the negative control was counted one and those of other groups were expressed as cell viability by comparing to the cell number of the negative control. In the implants without trehalose coating, with trehalose coating or in the bFGF-incorporated implant without trehalose coating, the cell viability was not significantly different. In the bFGF-incorporated implant with trehalose coating, the cell viability was significantly higher by 3.0 times of the negative control group. In the positive control group, the cell viability was increased to 7.0 times of the negative control group.

### ***Scanning electron microscope***

Fig. 1-4 shows SEM images of each implant. In the implant without trehalose coating, SEM observations showed microporous structure as shown Fig. 1-4 A. At a higher magnification, the crystal was typical spindle shape of hydroxyapatite with various sizes (Fig. 1-4 C). In the implant with trehalose coating, trehalose crystal covered the surface, and the crystallinity of the implant was not changed by trehalose treatment (Fig. 1-4 B and D).

### ***X-ray diffraction pattern***

The XRD pattern of the implants with or without trehalose coating is shown in Fig. 1-5. In the implant without trehalose coating, the observed position of diffraction lines was in agreement with the corresponding values for hydroxyapatite ( $\text{Ca}_{10}(\text{PO}_4)_6(\text{OH})_2$ ) and  $\alpha$ -TCP ( $\text{Ca}_3(\text{PO}_4)_2$ ) in all specimens, and additional peaks were detected due to other calcium phosphate components. The diffraction patterns showed no differences between trehalose-coated and trehalose-non-coated implants.

### ***Mechanical strength***

The compression strength was  $12.80 \pm 1.28$  MPa in the implant without treatment (control),  $13.79 \pm 1.53$  MPa in the implant with trehalose coating and  $9.10 \pm 1.48$  MPa in the implant with saline treatment, respectively. The compression strength of the implant with saline treatment was significantly lower than those of other implants ( $P < 0.05$ ). There was no significant difference between the control and the implant with trehalose coating (Fig. 1-6).

The bending strength was  $6.72 \pm 1.68$  MPa in the control,  $6.74 \pm 1.55$  MPa in the implant with trehalose coating and  $5.49 \pm 0.89$  MPa in the implant with saline-treatment,

respectively. The bending strength of the implant with saline treatment was significantly lower than those of other implants ( $P < 0.05$ ). There was no significant difference between the control and the implant with trehalose coating (Fig. 1-7).

## Discussion

Various types of bone implants incorporating bone growth factors have been reported (Komaki *et al.* 2006; Tazaki *et al.* 2009). Though calcium phosphate is a good material as a DDS, the property of releasing proteins is poorer than other artificial bone materials (Midy *et al.* 1998). Generally, the releasing rate of these growth factors is depending on crystallinity of the calcium phosphate, sintered temperature, affinity to  $\text{Ca}^{2+}$  ion and pH of the environment surrounding bone implants (Wassell *et al.* 1995; Ziegler *et al.* 2002; Matsumoto *et al.* 2004; Seshima *et al.* 2006). Dong *et al.* reported that bone morphogenetic protein (BMP) binds to  $-\text{OH}$ ,  $-\text{NH}_2$ ,  $-\text{COO}^-$  of hydroxyapatite and that this Coulomb force and hydrogen bond may play an important role in releasing BMP from the implant (Dong *et al.* 2007). However, the bind affinity of bFGF to calcium phosphate has not been reported. Onuma *et al.* reported that the binding affinity of bFGF to calcium phosphate is depending on pH and presence of NaCl (Onuma *et al.* 2004). However, this information may not be enough to estimate the releasing of bFGF from the calcium phosphate implant. It is also reported that bFGF is difficult to be released from calcium phosphate crystal in the physiological pH condition (Matsumoto *et al.* 2004; Niedhart *et al.* 2004).

In this study, I predicted that the bFGF was difficult to be release from the calcium

phosphate implant. From the results of *in vitro* cell proliferative experiment, there was no significant difference in cell viability between the control group and the bFGF-incorporated implant without trehalose coating groups, suggesting the difficulty in releasing bFGF from this implant used in this study.

According to the findings that cell viability under culture with implants with or without trehalose coating was not different, trehalose did not affect the osteoblastic cell proliferation. In the bFGF-incorporated implant with trehalose coating, the cell viability was significantly higher than that of the bFGF-incorporated implant without trehalose coating. This result may indicate that the trehalose coating to the implant enabled more bFGF releasing through direct binding inhibition of bFGF to calcium phosphate by trehalose.

The various mechanisms of trehalose function have been proposed, such as stabilization of the cell membrane through hydrogen-bonding, vitrification or switching off capability (Sum *et al.* 2003; Willart *et al.* 2006; Minutoli *et al.* 2008). SEM and XRD revealed that trehalose successfully covered the surface of the implant without changing crystallinity and basic characteristics. This phenomenon may be related to inhibition of the binding of bFGF to calcium phosphate.

Calcium phosphate crystallinity is considerably changed by sintered temperature and

pressure, chemical response and environmental hydrogen ion concentration because of electrolytic instability. Calcium phosphates tend to be stable as the form of hydroxyapatite (Suda. T 2007). When  $\alpha$ -TCP is dissolved,  $\alpha$ -TCP supplies  $\text{Ca}^{2+}$  and  $\text{PO}_4^{3-}$  into the liquid at the hydration phase. Then the solution becomes supersaturated with apatite, leading to the formation of spindle shaped crystals of hydroxyapatite. These hydroxyapatite crystals connected each other to form a set mass (Ishikawa *et al.* 1995; Ishikawa *et al.* 1995; Miyamoto *et al.* 1995). Subsequently, although the tailor-made implant was fabricated from pure  $\alpha$ -TCP, the main component of tailor-made implant was hydroxyapatite with  $\alpha$ -TCP in XRD. This component seemed not changed when the implant was coated with trehalose, indicating that trehalose may not influence on components of the implant.

When bFGF was released from calcium phosphate, the structure of bFGF may be degraded and its bioactivity could be decreased, (Ziegler *et al.* 2002). In this study, released bFGF from trehalose-coated implants could significantly proliferate the osteoblastic cells, indicating the following two hypothesis. (1) Trehalose may prevent degradation of released bFGF. Trehalose can bind to bFGF protein and preserve its structure (Liao *et al.* 2002). Le Nihouannen *et al.* reported trehalose could stabilize the bioactivity of proteins adsorbed to calcium phosphate (Le Nihouannen *et al.* 2008). (2)

Degradation may not decrease bioactivity of bFGF. Actually, bFGF incorporated to the calcium phosphate implant showed enough bioactivity in many studies (Martin *et al.* 1997; Alam *et al.* 2007).

It is one of the problems of calcium phosphate implants that they become fragile when soaked with body fluid or blood. The reason of this phenomenon be due to  $\text{Ca}^{2+}$  dissolution to the environmental solution (Liu *et al.* 2003). In this study, the bending and compression strength of the implant soaked with 0.9% saline significantly decreased than that of the control group, while mechanical strength of implants coated with trehalose did not decrease. This result may indicate that trehalose inhibited dissolution of  $\text{Ca}^{2+}$  ions from the implant.

In conclusion, trehalose-coated tailor-made implants could inhibit binding of bFGF to calcium phosphate, leading to earlier release of bFGF to proliferate osteogenic cells. In addition, trehalose coating also prevent the decrease in mechanical strength of the implant, potentially through suppression of dissolution of  $\text{Ca}^{2+}$  ion from implants.

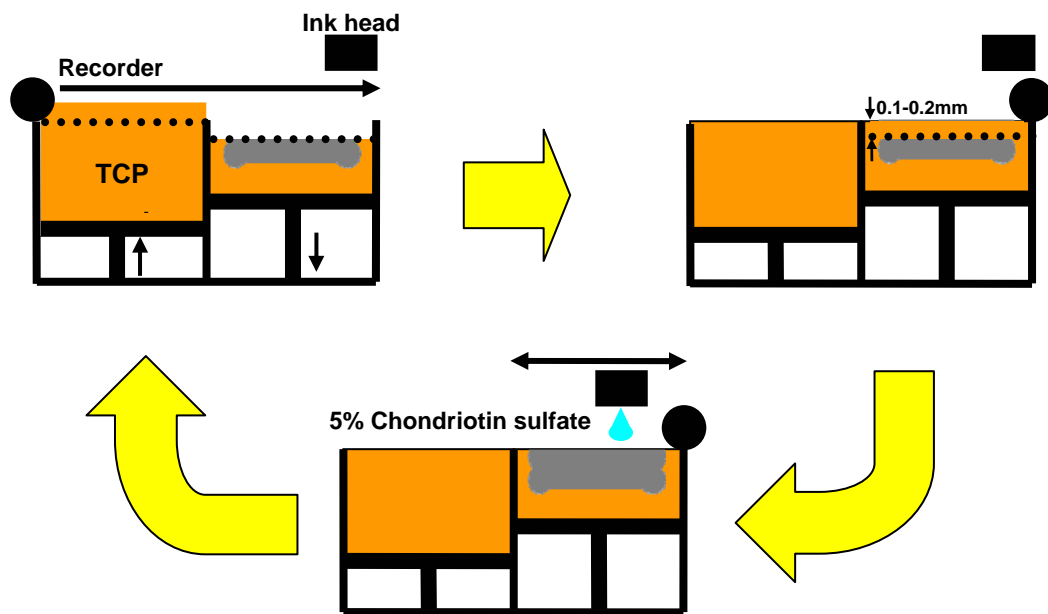


**Fig. 1-1** The process of fabrication of tailor-made implants using an ink-jet printer. Liquid binder, 5% chondroitin sulfate, 12% disodium succinate and 83% distilled water was ejected from the ink head to the thin sheet of  $\alpha$ -TCP powder, then this hardened sheet was piled repeatedly to make a solid implant. (TCP: tricalcium phosphate)

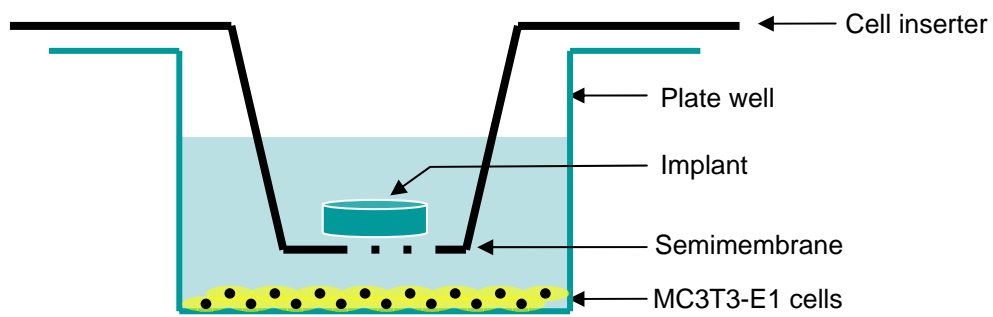


**Fig. 1-2** Culture method for evaluation of the effect of the implant with or without bFGF on the cell proliferation.

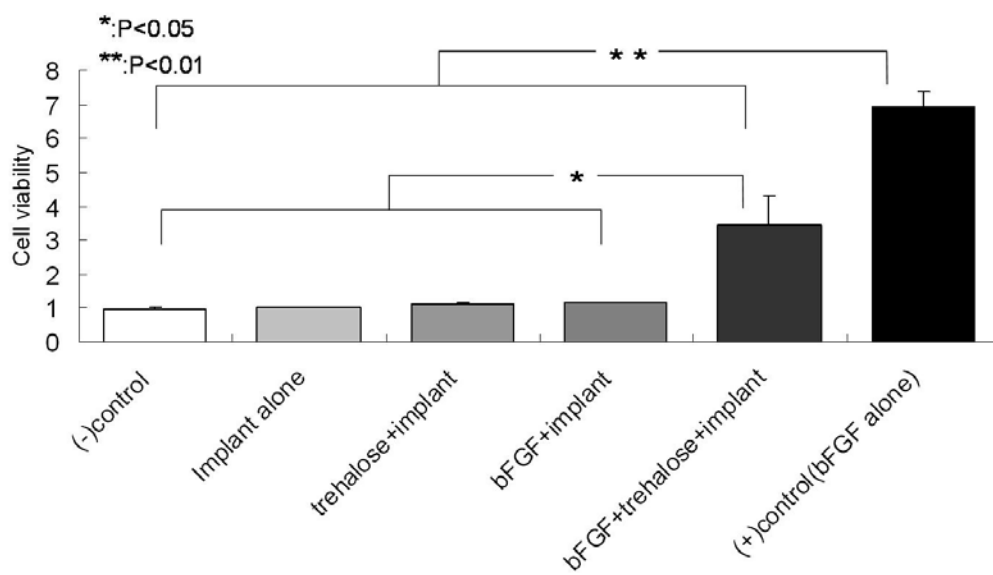


**Fig. 1-3** The result of cell proliferation test. bFGF and 5% trehalose-treated tailor-made implant group was showed significantly higher cell proliferation ratio than other groups except the positive control.

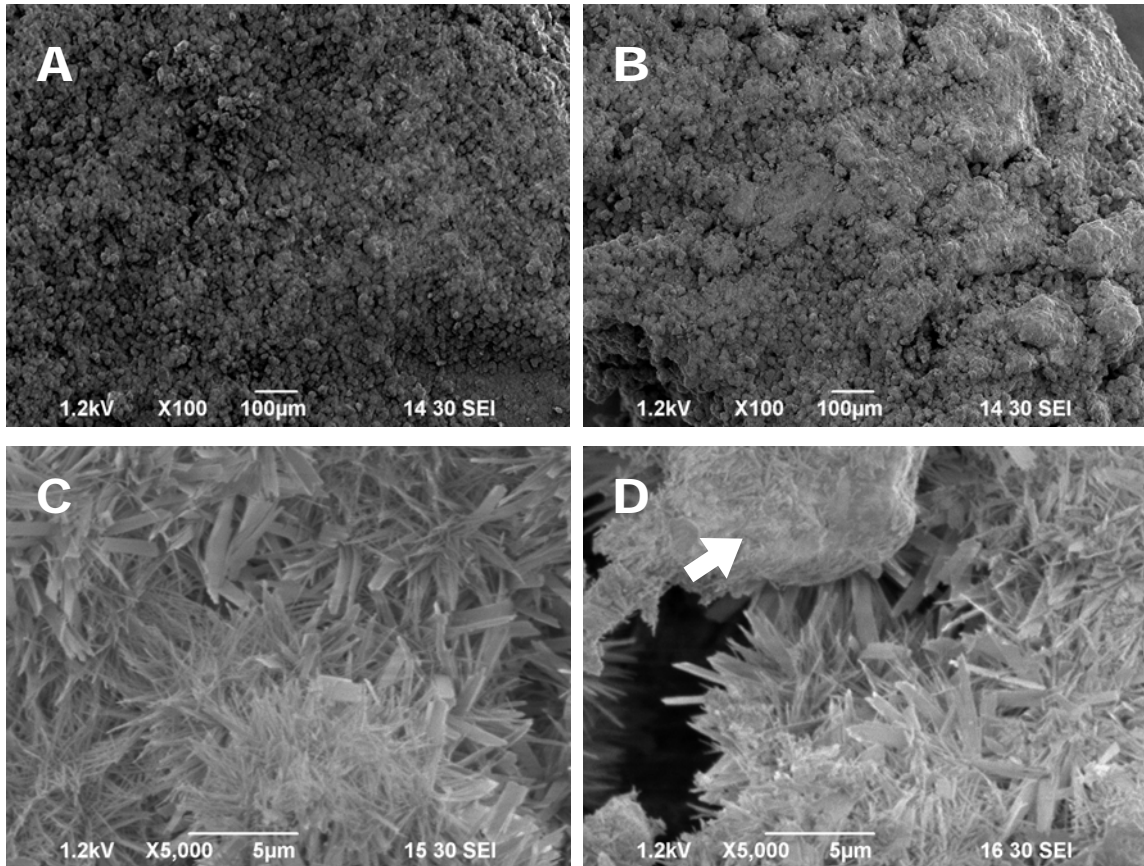


**Fig. 1-4** SEM images of the implant without trehalose coating (A, C) and with trehalose coating (B, D). The surface of the implant without trehalose coating was microporous and had spindle shaped crystals (A, C). The surface of the implant with trehalose coating was covered with trehalose crystal (white arrow) (B, D), and the structure of the spindle shaped crystal was maintained (D).

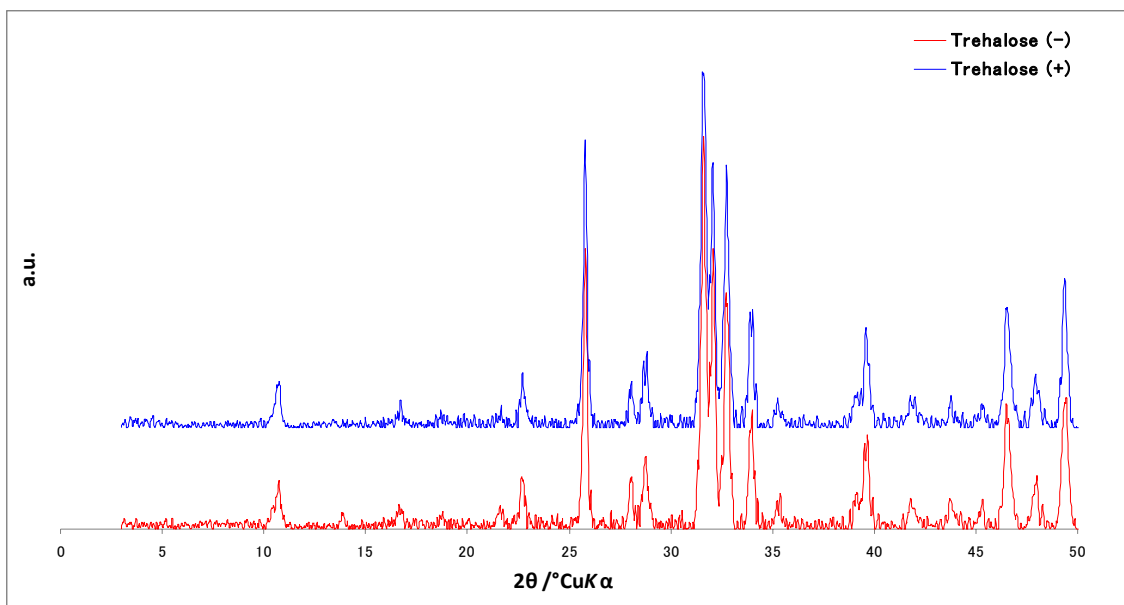


**Fig. 1-5** X-ray diffraction pattern. In the implant without trehalose coating, typical patterns of hydroxyapatite and  $\alpha$ -TCP were shown. There were no differences between trehalose-non-coated and trehalose-coated implants.

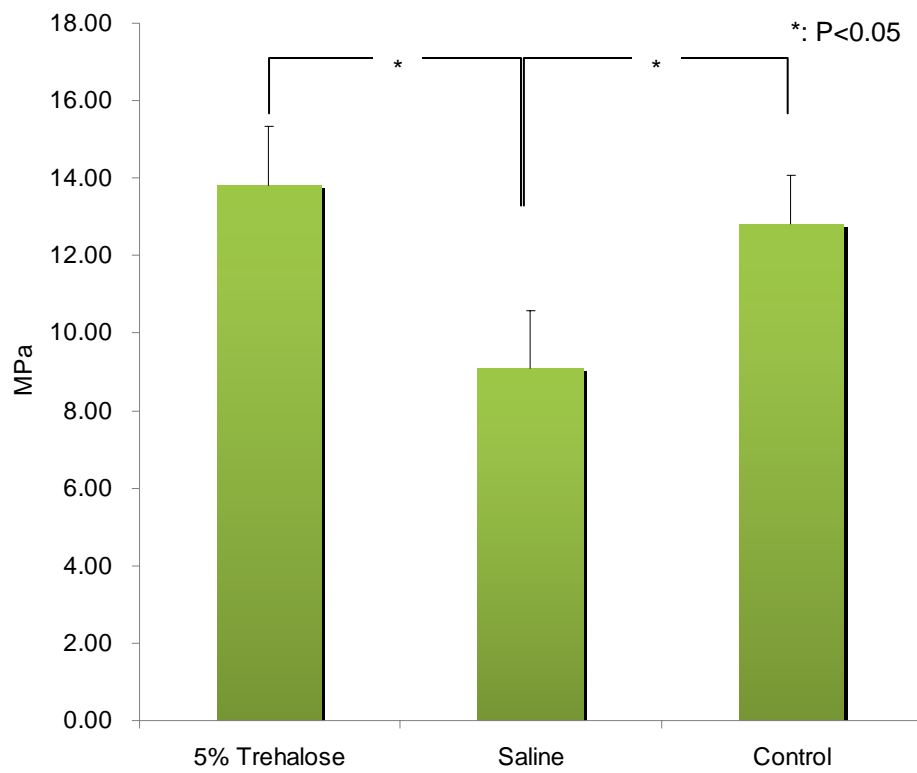


**Fig. 1-6** Maximum compression load strength of each implant. Strength of the saline-treated implant was significantly lower than that of the trehalose-treated and control implants ( $P < 0.05$ ).

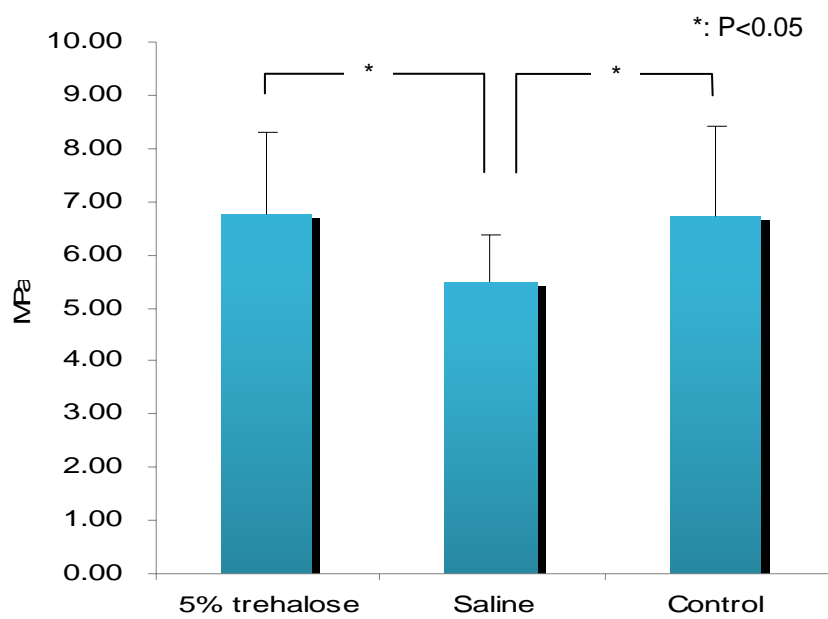


**Fig. 1-7** Maximum bending load strength of each implant. Strength of the saline-treated implant was significantly lower than that of the trehalose-treated and control implants ( $P < 0.05$ ).

**Chapter 2. Bone regeneration by implantation of  
bFGF-incorporated tailor-made implants with  
trehalose coating on the defect of the skull in dogs**

## Introduction

$\alpha$ -TCP and hydroxyapatite are biocompatible and osteoconductive materials (Jarcho 1986; Hollinger *et al.* 1996; Moore *et al.* 2001). These materials have been used for bone defect filler in the clinical practice (Cook *et al.* 1986; Kent *et al.* 1986). However, it is technically difficult to implant them to the bone defect due to their fragility and dispersion (Desjardins 1985; Propper 1985). Therefore, they are currently used in the paste form because of their self-setting ability (Koshino *et al.* 1995; Comuzzi *et al.* 2002; Tanag *et al.* 2006; Nakadate *et al.* 2008).

bFGF promotes the proliferation and differentiation of the osteoblastic cells *in vitro* (Hauschka *et al.* 1986; Gospodarowicz 1990), and induces the bone healing in the bone defect *in vivo* (Wang *et al.* 1996; Clarke *et al.* 2004). It is also known that bFGF stimulates bone formation depending on their dose *in vivo* (Draenert *et al.* 2009). A single injection of bFGF induced the systemic bone enhancement (Wronski 2001), however, bFGF alone injected to the bone defects induced significantly less bone growth than injected with a carrier (Tabata *et al.* 1998). Therefore, a number of carriers were studied in order to improve the releasing rate of bFGF from carriers (Hayashi *et al.* 2007; Cao *et al.* 2009).

Compared to rodents, the larger mammals may need larger doses of bFGF to promote

the bone regeneration at the bone defects and the ideal dose of bFGF is influenced according to the type of carriers. Nakamura *et al.* reported that a single injection of 200  $\mu\text{g}$  bFGF accelerated fracture healing in dogs (Nakamura *et al.* 1998), and 200  $\mu\text{g}$  bFGF combined with  $\beta$ -TCP also promoted bone regeneration in dogs (Hosokawa *et al.* 2000). In addition, the gelatinous carrier with 30  $\mu\text{g}$  bFGF stimulated the bone growth in dogs (Murakami *et al.* 2003). However, the optimal dose of bFGF combined with the composition of hydroxyapatite and  $\alpha$ -TCP to promote the bone regeneration has not yet been clarified.

Some researchers proposed that calcium phosphate could not be used as a carrier for bFGF because of the low release kinetic of bFGF (Niedhart *et al.* 2004), but, I confirmed the *in vitro* effects of the bFGF release from the implant with trehalose coating in Chapter 1.

The purpose of this chapter is (1) to investigate the optimal dose of bFGF incorporated with the tailor-made implant in *in vivo*, and (2) to evaluate its bone regeneration effect.

## Materials & Methods

### *Preparation of implants*

**Implant fabrication:** The tailor-made implant was designed on 3D image using the software Mimics program (Materialise) as in Chapter 1. The implant in this chapter was round disc shape with 11 mm in diameter and 4 mm in height, and the side aspect of implant was inclined at a 7.5 degrees angle. At the side of the implant, two parallel cylindrical holes of 2 mm in diameter were created parallel to each other to facilitate blood vessel and regenerated bone invasion (Igawa *et al.* 2006). At the top of the implant, the landmark with 1 mm height, 1mm width and 11 mm length, was created to indicate the direction of the cylindrical holes (Fig. 2-1). The fabrication process was the same as in Chapter 1.

**Trehalose coating:** The fabricated implants were subdivided into trehalose-coating group and trehalose non-coating group. The coating process was the same as in Chapter 1.

**bFGF incorporation:** bFGF was diluted with deionized water to 0.1, 1, 10  $\mu\text{g}/\mu\text{l}$  solution, respectively. Implants were infiltrated to their side aspect and cylindrical holes inlet with each dose of bFGF solution using a micropipette. The total dose of bFGF incorporated to one implant was 1, 10, 100 and 200  $\mu\text{g}$ , respectively. In the control

group, only deionized water was dropped in the same manner. Fig. 2-2 shows experimental grouping. All the implants were dried after soaking at room temperature.

### ***Experimental animals***

Ten female beagle dogs with the body weight from 8.3 kg to 10.7 kg (mean 9.4 kg) and the age from 1 year to 5 years were purchased from Nosan Corporation (Yokohama, Japan). Before starting the experiment, all the animals were confirmed to be clinically healthy through physical examination, radiography, hematology and blood chemistry panel. The following experiments were conducted under the Guidelines of the Animal Care Committee of the Graduate School of Agricultural and Life Sciences, the University of Tokyo.

### ***Surgical procedures***

The dogs were fasted for 12 hours before the implantation. Atropine sulfate at 25  $\mu\text{g}/\text{kg}$  was subcutaneously injected as preanesthetic medication followed by midazolam (0.1mg/kg). Intravenous injection of propofol (6mg/kg) was used for induction and anesthesia was maintained with 1.0-2.5% isoflurane and oxygen after the tracheal intubation. Cefazolan (20mg/kg) was intravenously injected as a preoperative antibiotic.

Administration of 5-20 µg/kg/hr fentanyl hydrate as an analgesic was started using a syringe pump at the time of induction of anesthesia and continued for 24 hours post-operatively.

During the surgery, hyperventilation was continued using a ventilator to maintain EtCO<sub>2</sub> at about 30 mmHg to prevent brain edema. The fluid therapy was performed with 10 ml/kg/hr lactated Ringer`s solution. ECG, EtCO<sub>2</sub>, SpO<sub>2</sub>, indirect blood pressure, respiration rate and body temperature were monitored during the surgery. To prevent the seizure after implantation, the dogs were intramuscularly injected with phenobarbital (2mg/kg) and dexamasone (1mg/kg) before the end of surgery.

Oklund`s bone defect model was used in this study (Oklund *et al.* 1986). The head was clipped and aseptically prepared with chlorhexidin and povidon-iodine. The midline of the head skin and subcutaneous tissues were incised. Bilateral temporalis muscles and fascia were incised curvedly, and bluntly dissected carefully from the temporal bone using a periosteal elevator. Four round bone defects of 11 mm in diameter were created using a perforator (Stryker Instruments, Kalamazoo, USA) to avoid the injury of the dura mater and surrounded periosteum. Two defects were located cranially and 2 defects caudally 2 cm at 4 cm and 2 cm from the external occipital protuberance, respectively, and bilaterally at 2 cm from the external sagittal crest. Four

implants of different regimen in a dog were assigned to each of defects (n=4; Fig. 2-3).

After implantation, the temporalis muscle, fascia, subcutaneous tissues and dermis were sutured in a continuous suture pattern with 3-0 or 4-0 polydioxanone. The skin was closed interruptedly with 3-0 nylon. For postoperative care, 15µg/kg buprenorphine and subcutaneous 20mg/kg cefazolan was injected intramuscularly twice a day for 3days. To prevent seizure and brain edema after implantation, intravenous dexametasone (0.5mg/kg on the first day, 0.25mg/kg on 2nd day, 0.13mg/kg on 3rd day) and 0.5g mannitol injection and 2mg/kg phenobarbital intramuscular injection were performed for 3 days. When dogs showed seizure, midazolam 0.5mg/kg was intravenously injected.

### ***Computed tomography (CT)***

CT was conducted to evaluate the new bone formation inside the cylindrical holes and around the implant immediately after the surgery and 2 and 4 weeks of implantation under the sedation with midazolam (0.3mg/kg, IM) and medetomidine (20ug/kg, IM) using a 4-channel multi detector CT equipment (Asterion TSX-021B, Toshiba, Tokyo, Japan) with 0.5mm slice thickness under the conditions of 120 kV and 180 mA.

### ***Gross evaluation***

At 4 weeks of implantation, the dogs were euthanatized with KCl injection under deep anesthesia with thiopental sodium at 30mg/kg. The implant and surrounded tissues were grossly observed carefully and excised using a sagittal saw (Osada Electronics, Tokyo, Japan).

### ***Micro-CT***

A desktop X-ray micro-CT system (Shimadzu, SMX-90CT, Kyoto, Japan) was used to evaluate the regenerated bone of excised tissues. The excised tissues were scanned with X-rays generated by a sealed micro-focus X-ray tube at 90 KV and 110  $\mu$ A. The sections were scanned in z-axis, and the scanned data were virtually reconstructed parallel to cylindrical holes of the implants in order to observe the regenerated bone formation within the cylindrical holes using micro-CT analysis program (TRI/3D-VIE, RATOC, Tokyo, Japan).

### ***Histology***

Excised tissues were fixed with 10% neutered formalin (WAKO, Tokyo, Japan) for 5 days, and decalcified with 10% ethylenediaminetetraacetic acid (EDTA; WAKO, Tokyo,

Japan) solution for 4-5 months. Decalcifying solution was changed every 3-4 days. Decalcified tissues were trimmed parallel to the cylindrical holes and embedded in paraffin. The tissue block was cut into 7- $\mu$ m thick sections, and stained with Masson's trichrome after deparaffinization. The stained sections were examined under a light microscope and measured the area of regenerated bone using image J software (US National Institutes of Health, Bethesda, Maryland, USA).

### ***Statistical analysis***

The mean values and standard deviations of area of the regenerated bone were calculated, and student t-test was performed using spreadsheet program (Excel, Microsoft corporation, USA). P-value less than 0.05 was considered to be statistically significant.

## **Results**

Five out of 10 dogs showed mild seizure 0 – 1 day after the surgery, but immediate sedation with midazolam was effective to stop the clinical signs. There were not severe problems nor other clinically abnormal signs during the whole observation period.

### ***Gross evaluation***

Fig. 2-4 shows gross findings of all the groups. All the implants of all groups were well fitted and connected to the surrounding tissue, and there were not any abnormal findings around the implants such as inflammation or infection. Grossly, there seemed no difference in new bone formation and bone union between trehalose coating groups and non-coating groups. On the contrary, it seemed that bFGF influenced the new bone formation dose-dependently. In 100 and 200 µg bFGF groups, more new bone formation from the surrounding periosteum than that in 0, 1 and 10 µg bFGF groups was observed, and the heterotopic bone regeneration was found in the 200 µg bFGF group. (Fig. 2-5)

### ***CT images***

Any displacement and breakage of the implants were not observed in all the dogs during the whole observation period. Fig. 2-6 showed the typical CT images in all the

groups during the 4 weeks after implantation. At 2 weeks of implantation, there were no changes in CT images among all groups. At 4 weeks of implantation, the new bone formation was observed in the cylindrical holes and around the interface between implants and skull bones. This new bone formation was observed more or less in all the groups, but the quantity of the bone seemed dose-dependent. In 100 and 200  $\mu\text{g}$  bFGF groups, more and massive bone formation than that of 0, 1 and 10  $\mu\text{g}$  bFGF groups. Significant difference was not observed between trehalose coating groups and non-coating groups.

### ***Micro-CT images***

On micro-CT images, there was no difference in new bone formation between implants with and without trehalose coating. In 0, 1 and 10  $\mu\text{g}$  bFGF groups, there was only a little mineralized tissue within the cylindrical holes, while in 100 and 200  $\mu\text{g}$  bFGF groups, there were massive mineralized tissues from the surrounding periosteum to the cylindrical holes (Fig. 2-7).

### ***Histological findings***

Fig. 2-8 shows histological findings of all the groups. There seemed no difference in

bone regeneration at any areas of implants between those with and without trehalose coating. In implants with 100 and 200  $\mu\text{g}$  bFGF, massive regenerative bone tissues were formed from the surrounding periosteum to the cylindrical holes as shown in micro-CT. Fig. 2-9 shows the findings with high magnification of implants with 10  $\mu\text{g}$  and 100  $\mu\text{g}$  bFGF without trehalose coating. In 100  $\mu\text{g}$  bFGF-incorporated implant without trehalose coating group, there were more regenerated bones at the surrounding periosteum than in 10  $\mu\text{g}$  bFGF one without trehalose coating group.

Fig. 2-10 shows the measurement of the area of regenerated bones in all groups. The area of regenerated bones in implants with 0, 1 and 10  $\mu\text{g}$  bFGF with or without trehalose coating was similar. In implants with 100 and 200  $\mu\text{g}$  bFGF of the trehalose non-coated groups, the area of regenerated bones was significantly higher than those with 0, 1 and 10  $\mu\text{g}$  bFGF of trehalose non-coated groups, however in implants with 100 and 200  $\mu\text{g}$  bFGF of trehalose coating implant groups, there were no significances when compared to those with 0, 1 and 10  $\mu\text{g}$  bFGF of trehalose coating groups. Between the trehalose-coated implant and non-coated implant at any doses of bFGF, there were also no significant differences.

## Discussion

Five dogs showed mild seizure after the surgery in this study, probably due to the invasive skull surgery which may induce brain edema, not toxicity of the tailor-made implant. In the previous paper, using the same implant, there were no harmful effect on the implantation sites (Igawa *et al.* 2006).

In Chapter 1, it was indicated that the bFGF release from the trehalose non-coated implants was suppressed *in vitro*. However, in the results of this chapter, it seemed no difference in bone regeneration between implants with and without trehalose coating. The cause of this phenomenon may be explained as follows.

When a trehalose-non-coated implant was implanted *in vivo*, proteins or other blood components may bind to implants and may induce the inhibition of bFGF binding to the calcium phosphate, the similar effect of trehalose coating. It was reported that the protein, such as albumin, can bind to calcium phosphate easily (Wassell *et al.* 1995). Although the binding affinity of these proteins and bFGF to calcium phosphate is not known, they may displace bFGF bound to the implant. In addition, electrolytes of the body fluid may interfere  $\text{Ca}^{2+}$  dissolution from the implant. In the *in vivo* condition, negative ions of electrolytes attached to implants may bind to  $\text{Ca}^{2+}$  through hydrogen bond, and  $\text{Ca}^{2+}$  dissolubility may be increased. Therefore, bFGF bound to  $\text{Ca}^{2+}$  may be

decreased through  $\text{Ca}^{2+}$  dissolubility.

bFGF can induce promotion of bone healing *in vivo* (Thoren *et al.* 1993). Even a single injection of bFGF has been demonstrated to promote bone healing in the bone fracture model of rats, rabbits, dogs and monkeys (Kato *et al.* 1998; Nakamura *et al.* 1998; Kawaguchi *et al.* 2001; Nakajima *et al.* 2007). However, the bFGF-incorporated carrier implantation may show more bone regeneration than a single injection (Tabata *et al.* 1998; Oi *et al.* 2009). Various types of carriers incorporating bFGF have been studied. The gelatin incorporated with 30  $\mu\text{g}$  bFGF was shown to produce more regenerated bone than the gelatin alone in mandibular bone defects of dogs (Murakami *et al.* 2003). The collagen minipellet containing 0.15  $\mu\text{g}$  bFGF has also shown higher regenerated bone production (Hosokawa *et al.* 2000). However, the optimal dose of bFGF incorporated to the carrier may be depending on the material of the carrier.

In this chapter, I tried to define the optimal dose of bFGF incorporated to tailor-made implants in dogs. When compared to the lower doses, 100 and 200  $\mu\text{g}$  bFGF showed significantly more bone regeneration in dogs. It is known that the effect of bFGF on bone regeneration is dose dependent (Wang *et al.* 1996). In this study, there was no significant differences between 100 and 200  $\mu\text{g}$  bFGF groups in both gross finding and histological evaluations, and moreover, heterotopic regenerated bone was observed in

implants with 200  $\mu\text{g}$  bFGF groups. It may be indicate that bFGF was supersaturated in the surface of the tailor-made implant and moved to the heterotopic region of the skull in 200  $\mu\text{g}$  bFGF group. The outflow of bFGF to the heterotopic region may not be ideal for the implant, because the heterotopic regenerated bone could show harmful effects on the recipient, and it will take a long time to return to the normal bone shape through remodeling. In addition, excess doses of bFGF in the bone defect could inhibit the osteoblast differentiation (Mansukhani *et al.* 2000). Oi *et al.* reported that the combination of  $\beta$ -TCP and 200  $\mu\text{g}$  bFGF showed promotion of the regenerated bone in dogs (Oi *et al.* 2009). In this chapter, even lower doses of bFGF incorporated to the implants promoted the bone regeneration, indicating that the tailor-made implant could be a more effective carrier than  $\beta$ -TCP. From the results of this study, 100  $\mu\text{g}$  bFGF for the tailor-made implant of this size may be optimal.

In this chapter, most of the regenerated bone was oriented from the periosteal membrane of the surrounding bone. The periosteum has bone lining cells which consist of the osteoprogenitor cells (Suda 2007). According to the histological findings, it is considered that bFGF mainly induced bone regeneration from the sites where the osteogenic cells were rich.

In conclusion, it was confirmed that the bFGF-incorporated tailor-made implant with

trehalose coating is biocompatible to dogs. In addition, 100 µg bFGF was considered to be the effective dose for incorporation to this implant. Although there was no effect of trehalose coating, in order to the protein stability and maintenance of the mechanical strength of the implant, trehalose coating to the tailor-made implant may be preferred for the clinical application.

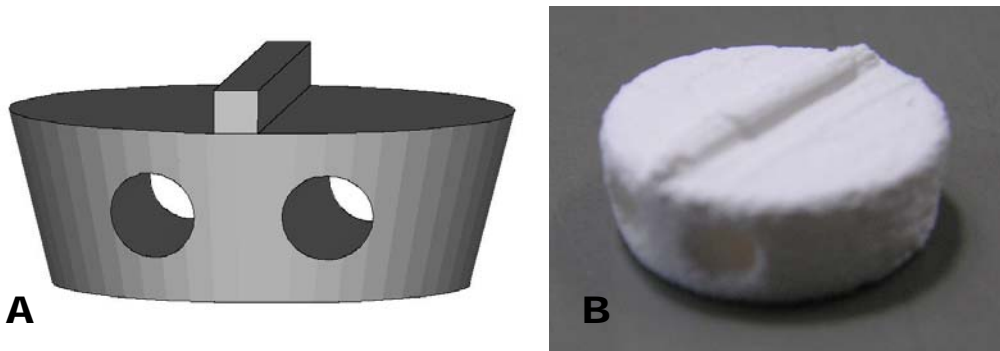


**Fig. 2-1** CAD data of implant (A) and a fabricated implant (B). The implant had two cylindrical holes to facilitate the blood vessels and the regenerated bone invasion.

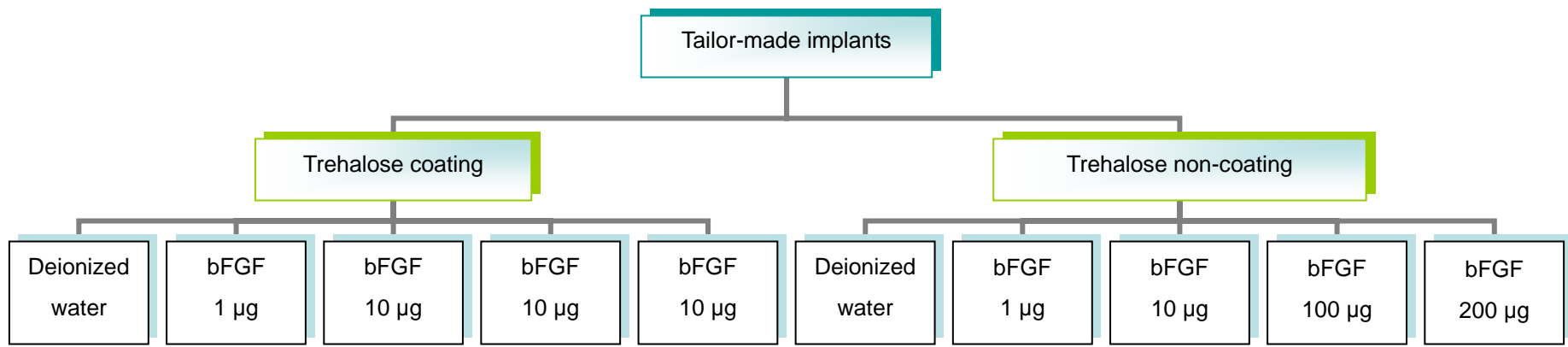


**Fig. 2-2** Experimental groups of implants with or without trehalose coating and with different doses of bFGF



**Fig. 2-3** Four bone defects were created at the temporalis bone. In one dog, 4 implants of different regimen were assigned to each of the defects.

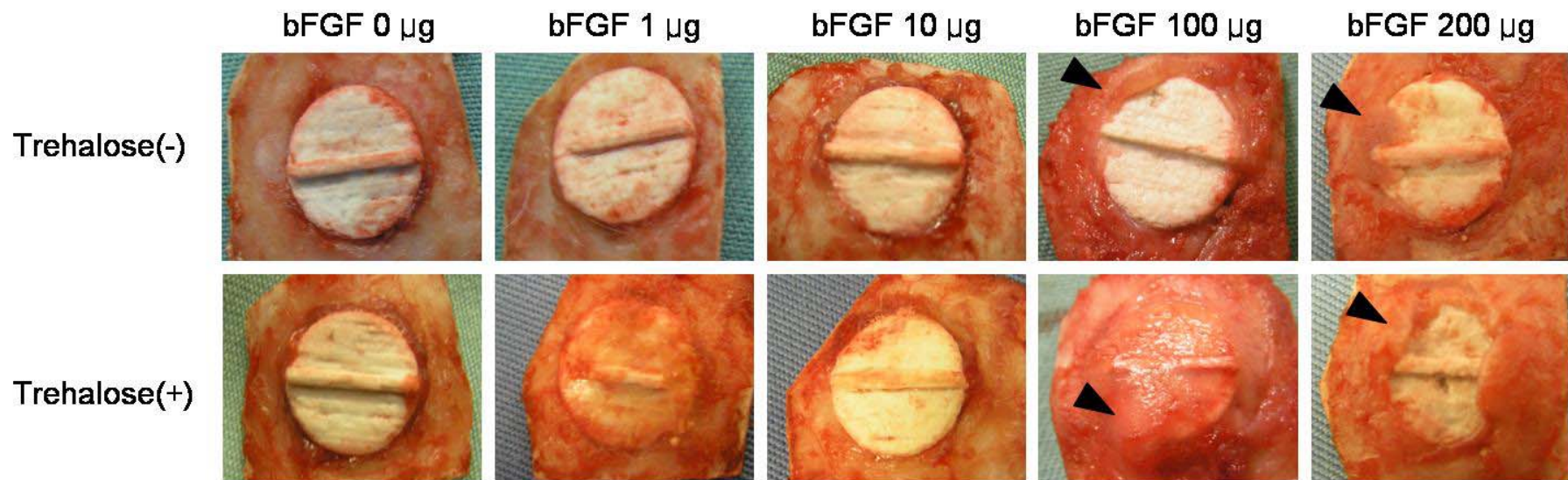


**Fig. 2-4** Gross findings of all groups at 4 weeks of implantation. There was no difference in new bone formation between implants with or without trehalose coating. Groups of bFGF at 100 and 200  $\mu\text{g}$  showed massive new bone formation from the surrounding periosteum (black arrow head).

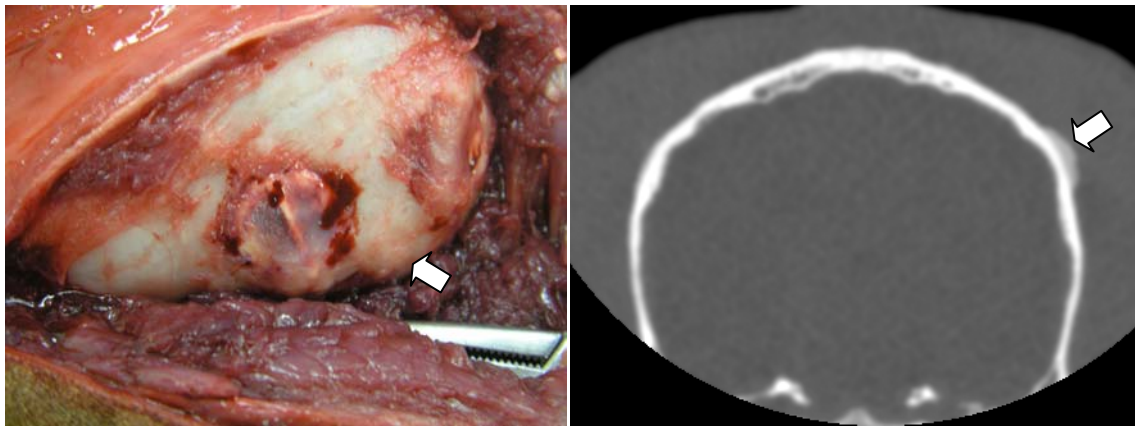


**Fig. 2-5** The heterotopic bone formation (white arrows) was observed at the bone surface near the 200  $\mu$ g bFGF-incorporated implant.

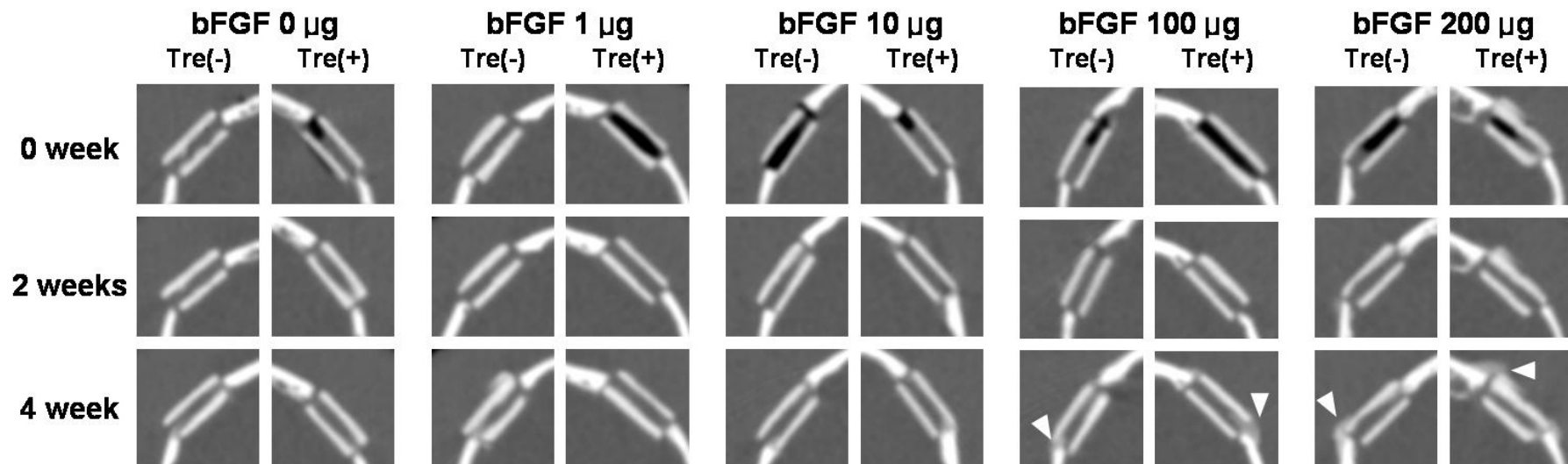


**Fig. 2-6** CT images of implants and the surrounding bone tissues 0, 2 and 4 weeks after implantation. There seemed no difference in bone formation in the cylindrical hole and surround the implants between trehalose-coated and non-coated groups. More new bone formation was observed in 100 and 200  $\mu$ g bFGF groups at 4 weeks after implantation (white arrow head).

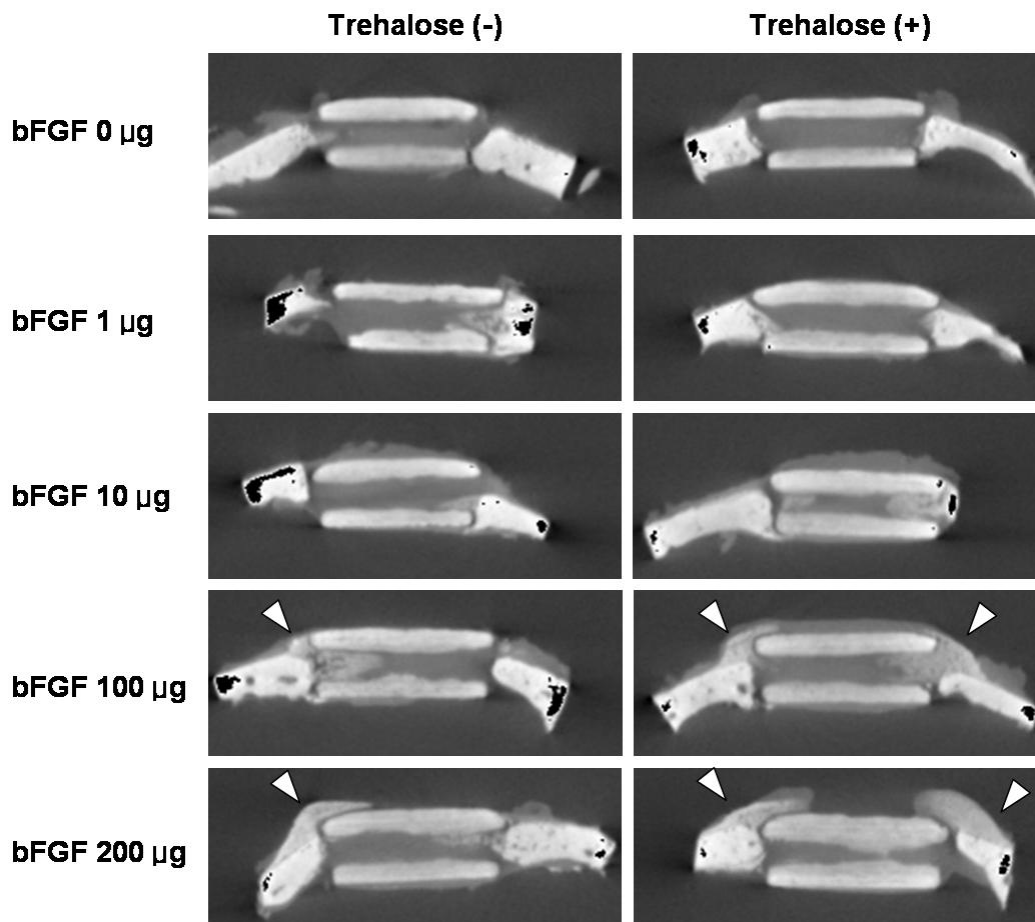


**Fig. 2-7** The micro-CT images. There were massive mineralized tissues (white arrow head) from the surrounding periosteum to the cylindrical holes in implants incorporated with 100 and 200  $\mu$ g bFGF.

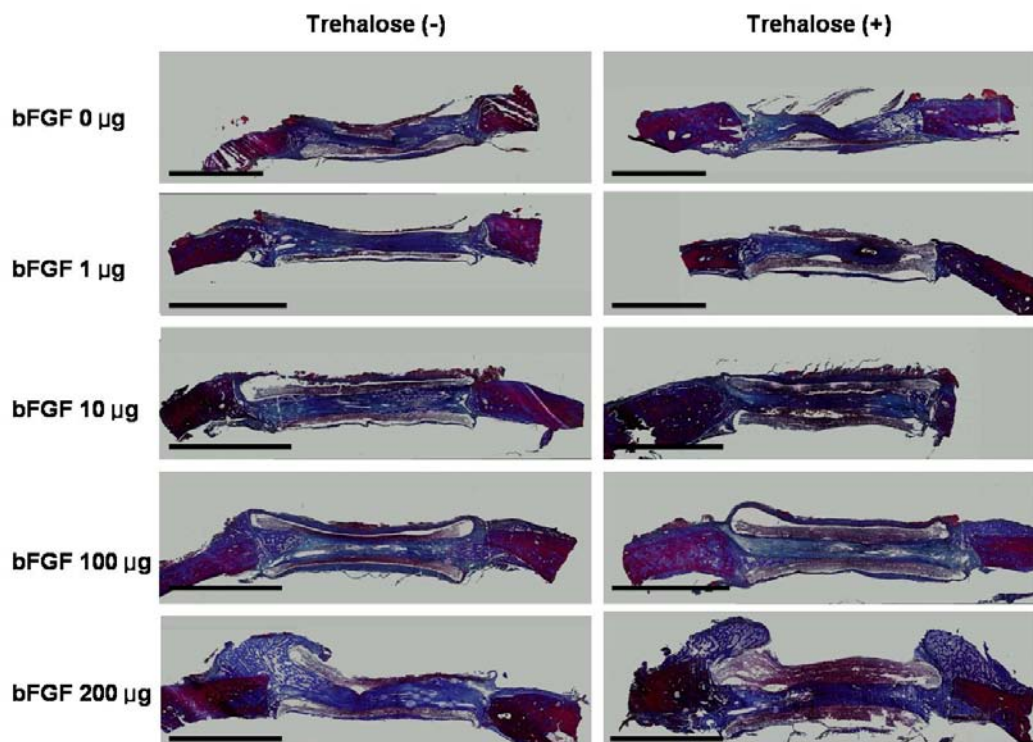


**Fig. 2-8** The histologic findings of all groups. There were massive regenerated bones from the surrounding periosteum to the cylindrical holes in implants incorporated with 100 and 200  $\mu$ g bFGF. (Masson trichrome stain, scale bar: 10mm)

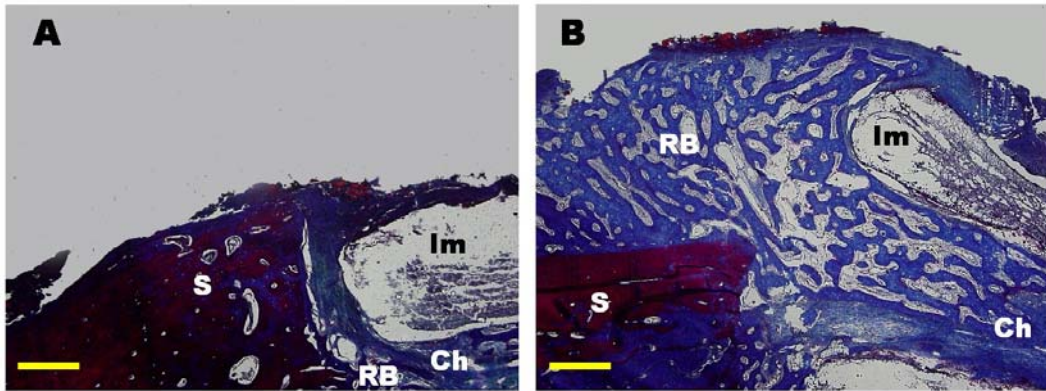


**Fig. 2-9** High magnification of the histological findings. (A) the 10 µg bFGF-incorporated implant without trehalose coating, (B) the 100 µg bFGF-incorporated implant without trehalose coating group (S: skull, Im: the body of implant, RB: regenerated bone, Ch: cylindrical holes; scale bar: 1mm)

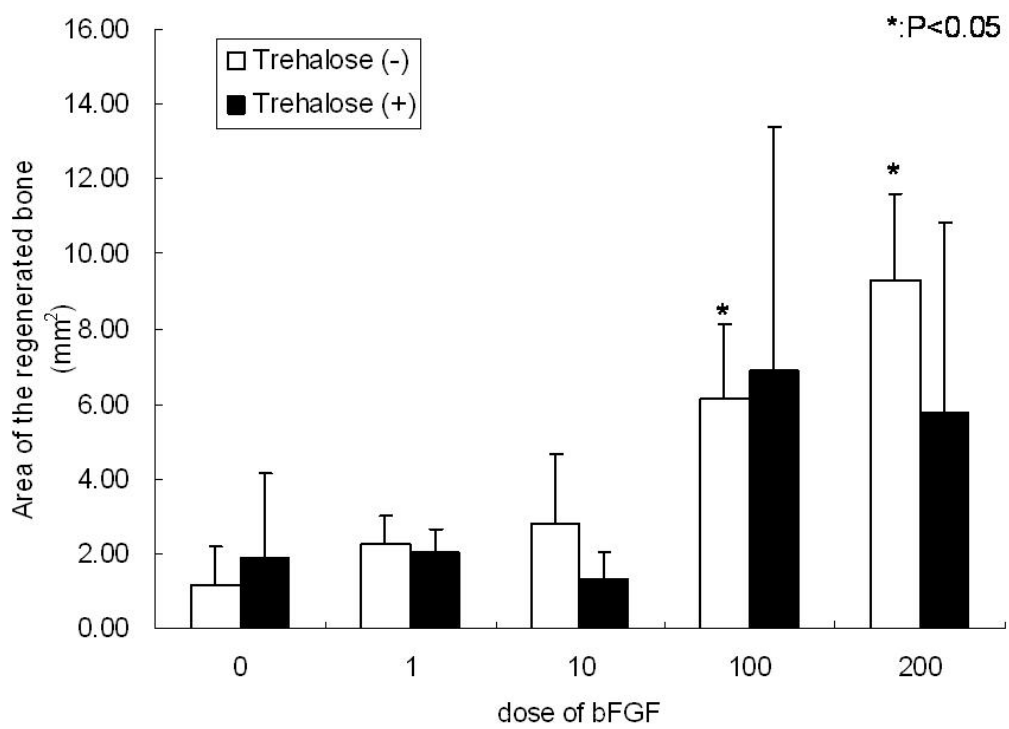


**Fig. 2-10** The area of regenerated bones. There was no significant difference between implants with and without trehalose coating at any bFGF doses. Implants with 100 and 200 µg bFGF of the trehalose non-coating groups showed significantly higher areas than those with 0, 1, 10 µg bFGF of the trehalose non-coated groups ( $P < 0.05$ ).

**Chapter 3. Long-term effectiveness of trehalose-coated and bFGF-incorporated implants for critical size defect of the skull of dogs**

## **Introduction**

The healing process of the bone defects is accomplished by the differentiation of the osteoblasts and osteoclasts, then the remodeling process through these cells. However, in case that the size of bone defects is exceeding a certain level, repairing process may be interrupted (Denny *et al.* 2000; Millis *et al.* 2001; Cheung 2005). Critical size defect (CSD) is defined as the smallest size of the intraosseous wound in a particular bone and species of animal that will not heal spontaneously during the lifetime of the animal. Repairing process of the CSD results in the formation of fibrous connective tissue rather than bone (Schmitz *et al.* 1986).

CSD has been widely used experimentally in the evaluation for the function of the implant incorporated with osteoinductive factors and osteogenic cells (Damien *et al.* 1994; Sweeney *et al.* 1995; Kamakura *et al.* 2001; Cowan *et al.* 2004). For complex anatomical defects such as the skull defect, the implant should fit to the defect three-dimensionally and provide sufficient load bearing until the time of the bone formation. The implant should also have a function as a DDS to promote the bone regeneration (Hollister *et al.* 2005).

In Chapter 2, the tailor-made implant may fulfill these requirements and be

successfully applied for the large bone defect of the skull in dogs. However, bone regeneration and remodeling generally takes a longer period to be accomplished especially in the larger defect.

The purpose of this chapter is to evaluate the dynamic changes of bone regeneration for a longer time period after implantation of the tailor-made artificial bone with and without bFGF to the CSD of the skull in dogs.

## **Materials & Methods**

### *Preparation of implant*

**Implant fabrication:** Computed tomography (CT) for the skull of 9 beagle dogs was performed under sedation, using a 4-channel multi detector CT equipment (Asterion TSX-021B, Toshiba). According to the CT data, bone implants with a round shape with 20 mm in diameter were created. In addition, I created a total of 6 cylindrical holes of 2 mm in diameter inside the implant: 3 cylindrical holes in the sagittal direction and 3 in the transverse direction (Fig. 3-1).

**Trehalose coating:** All fabricated implants were coated with 5% trehalose, as described in Chapter 1. Fabricated implants were autoclaved at 121 °C for 30 minutes. Implants were dried under pressure and preserved at room temperature until implantation.

**bFGF infiltration:** Since the circumference of the implant was twice larger than that used in Chapter 2, the dose of bFGF was determined as 200 µg per one implant. For bFGF-incorporated tailor-made implant with trehalose coating (fTI group), 20 µl of bFGF solution (200 µg bFGF) was dropped to the lateral face including the inlet of cylindrical holes with a micropipette, and the implant was

dried for 10 minutes at room temperature. For the TI group without bFGF, deionized water instead of bFGF was dropped similarly for the tailor-made implant with trehalose coating.

### ***Experimental animals***

Four male and 5 female beagle dogs with the body weight from 8.3 kg to 10.7 kg (mean 9.4kg) and the age from 1 year to 5 years were purchased from Nosan Corporation. Physical examination, radiography for abdomen and thorax, complete blood count and blood chemistry analysis were performed before implantation.

All the experimental procedures using dogs were conducted under the Guidelines of the Animal Care Committee of the Graduate School of Agricultural and Life Sciences, the University of Tokyo.

### ***Surgical procedures***

Anesthetic procedures, protocols for prevention of seizure, aseptical preparation and the surgical approach to the skull were the same as in Chapter 2.

As the CSD model for the skull of dogs, the size of 20 mm has been proposed

(Amstutz *et al.* 1984; Schmitz *et al.* 1986). Two round defects with 20mm in diameter were created using round bur and a ronguer at the 30 mm cranial from the external occipital protuberance and 20 mm lateral from the external sagittal crest, avoiding the dura mater and the surrounded periosteum injuries. TI or fTI was implanted to these bone defects. As a negative control, the bone defects were unfilled (each group n=6; Fig. 3-2). Closure of the surgical wound and post operative care were similar to those in Chapter 2.

### ***Computed tomography***

CT was conducted to evaluate the new bone formation inside and around the implant and changes in the implant volume. The dogs were sedated using midazolam (0.3mg/kg, IM) and medetomidine (20ug/kg, IM), and CT scanning was performed immediately after the surgery and every 1 month until 6 months of the implantation, then every 2 months until 12 months of the implantation. Obtained CT data were converted CAD data using the software mimics, and the 3 dimensional volume of the implant involving the implant body and the regenerated bone within the cylindrical holes was extracted and measured.

### ***Gross evaluation at 12 months of implantation***

At 12 months of implantation, the dogs were euthanatized with 30 mg/kg thiopental sodium and KCl. The implant and surrounded tissues were observed carefully and excised using a sagittal saw.

### ***Micro-CT***

The micro-CT scanning process was the same as in Chapter 2. The section was scanned along z-axis and the scanned images were reconstructed along y-axis to observe the whole cylindrical holes. The regenerated bone within the cylindrical holes was reconstructed using micro-CT analysis program (TRI/3D-VIE, RATOC, Tokyo, Japan; Fig. 3-3).

After micro-CT scanning, 3 samples of each group were used for histology and fluorochrome stain, and the others were used for 3 point bending strength test.

### ***Histology***

Excised tissues were fixed with 70% ethanol for 4 days (n=3). Tissues were stained with Villanueva bone stain for 6 days (Villanueva 1974; Villanueva *et al.* 1989), dehydrated through ascending graded alcohols, defatted in an acetone and methylmethacrylate monomer mixture (mix ratio 1:2), and embedded in methyl

methacrylate (WAKO chemicals). Plastic blocks of cross sections with 200- $\mu\text{m}$  thickness were cut parallel to the cylindrical holes with a precision bone saw. Sections were mounted on plastic slides and ground to a thickness of 50  $\mu\text{m}$  using a precision lapping machine (Maruto, Tokyo, Japan), then manually ground according to the method of Frost (Frost 1958). The stained sections were examined under a light microscope and the sum of regenerated bones area in the bone defects (SRBA) and the sum of the original defect areas (SODA) were measured using image J software (US National Institutes of Health, Bethesda, Maryland, USA), then the ratio SRBA/SODA was calculated.

### ***Fluorochrome labeling and fluorescence microscopy***

Bone labeling was performed using 3 fluorochromes, oxytetracycline (Terramycin, Pfizer Incorporation, Seoul, Korea), calcein (Sigma-Aldrich, Tokyo, Japan) and alizarine complexone (Sigma-Aldrich) as fluorescent markers in the course of new bone formation.

Oxytetracycline (20mg/kg) was intravenously injected twice at 2 and 4 weeks of implantation, respectively (injected 4 times totally). Calcein (20 mg/kg) was prepared with sodium bicarbonate at pH 7.2 and sterilized through a millipore

filter with 0.22  $\mu\text{m}$  pore size, then intravenously injected twice at 2 weeks interval at 6 months of implantation. Alizarin complexone (20 mg/kg) was prepared similarly to that of calcein, and intravenously injected twice at 2 weeks interval at 12 months of implantation.

Tissues specimens were observed under a fluorescence microscope (Axiovert 200, Zeiss, Germany) and various types of fluorescence filter set (oxytetracycline: #18, calcein: #10, alizarin complexone: #20) were used for observation of fluorochrome labeling. Details of the wavelength are given in Table. 3-1 (Suzuki *et al.* 1966; Dhem *et al.* 1976; O'Brien *et al.* 2002).

### ***Three point bending strength***

Three point bending strength was measured for the samples of each group (n=3). As a normal control, the skull of the healthy cadaver dog was collected. Experimental samples were trimmed with the dimension of 30×40 mm and 3-point bending strength test was performed using INSTRON universal testing machine (Instron-3365, Instron Corporation) with a span size of 28 mm, load cell of 5kN and load speed at 1.0 mm/min.

### *Statistical analysis*

In the volume of the implant on CT image, the area of the regenerated bone on histology and mechanical strength, the mean and SD were calculated, and student t-test was performed using spreadsheet program (Excel, Microsoft). P value less than 0.05 was considered to be statistically significant.

## **Results**

Four dogs had mild seizure within a few days after the surgery of implantation and were sedated immediately treated with midazolam injection. There were no other clinically abnormal signs during the whole observation period.

### ***CT findings***

In the negative control group without the implant, little new bone formation was observed at the bone defects during the whole experimental period. On the contrary, in TI and fTI groups, the mineralized tissues were proliferated between the implant and the skull, leading to the increased volume of implant on CT. In addition, and the gap between skull and the implant was fully filled with mineralized tissues in fTI group (Fig. 3-4). The regenerated bone was formed at the surrounding periosteum at 1 month of implantation, but disappeared at 2 months of implantation in the fTI group (Fig. 3-5). No such regenerated bone formation was observed in the TI group. Fig. 3-6 shows the change in the calculated volume of implant on CT. The volume gradually increased in both TI and fTI groups, and the volume in the fTI group was significantly higher than that in TI after 2 months of implantation ( $P<0.05$ ) excluding 4 months of implantation.

### ***Gross evaluation***

At necropsy, the implants of TI and fTI groups were firmly attached to the skull without deformation or degeneration of the implant, and there were no inflammatory response at the implanted site. Grossly, the bone defect of negative control group was unfilled with any bone tissues, and the temporalis muscle adhered to the dura mater at the bone defect (Fig. 3-7).

### ***Micro-CT scanning***

Fig. 3-8 shows the inner structure of the cylindrical holes reconstructed along the y-axis of micro-CT images in each group. In the negative control group, no new bone formation was observed. While a few mineralized tissues within cylindrical holes were observed in the TI group, more mineralized tissues were observed in the fTI group.

### ***Histology***

Fig. 3-9 shows the typical histological findings of the implant and the surrounding tissues of each group. In the negative control group, the bone defect

was filled with muscles, and no regenerative bones were observed. On the contrary, the implants of the TI and fTI groups were well attached with the regenerated bones within the cylindrical holes, and more regenerated bone was observed in the fTI group than in the TI group (Fig. 3-9 B, C).

Fig. 3-10 shows SRBA and SRBA/SODA ratios of the TI and fTI groups. The SRBA was  $4.18 \pm 0.42 \text{ mm}^2$  in the TI group and  $8.98 \pm 0.30 \text{ mm}^2$  in the fTI group ( $P$  values = 0.06), respectively. The SRBA/SODA was  $11.62 \pm 0.33 \%$  in the TI group and  $24.71 \pm 3.23 \%$  in the fTI group, respectively, and the difference was statistically significant ( $P = 0.01$ ).

Fig. 3-11 shows the histological findings of the implant and surrounding tissues in the fTI groups. The matrix of the implant was partially replaced by the regenerated bone (Fig. 3-11 A). The outside surface of the implant of the TI and fTI groups was smooth and covered with the thin fibrous tissue or the dura mater without clear matrix replacement (Fig. 3-11 B,D), and the surface of the cylindrical holes was rough and resorbed by activated osteoclasts (Fig. 3-11 C). There were no remarkable differences between the TI and fTI groups.

### ***Fluorochrome labeling***

Three fluorochromes, oxytetracycline, calcein and alizarin complexone, were labeled to the bone tissues successfully (Fig. 3-12). In the negative control group, oxytetracycline-labeled bone tissue (blue label) was mainly observed as two concentric circles at the surface of bone defects and the endosteum of the skull. Calcein-labeled bone tissues (green label) existed inside of the blue label at the surface of bone defects. Alizarin complexone-labeled bone tissue (red label) was not clear in the negative control group.

In the TI group, the blue labeled bone tissue existed the site similar to the negative control group. The green double labeled bone tissue existed at the center of the regenerated bone within the cylindrical holes. The red label was also not clear in this group.

In the fTI group, most of regenerated bones were labeled with blue. The green labeled bone tissue existed at the surface of the regenerated bone and the implant. The red label was also not clear.

### ***3-point bending strength***

Fig. 3-13 shows the mean maximum load for bending stress in each group. The

mean bending strength was  $14.29 \pm 5.83$  kgf in the negative control group,  $12.47 \pm 6.66$  kgf in the TI group, and  $16.59 \pm 2.16$  kgf in the fTI group, respectively. The normal skull (the positive control) showed  $40.05 \pm 11.73$  kgf which was significantly higher than all experimental groups, and there was no significant difference among the 3 experimental groups.

## Discussion

In this chapter, the tailor-made implant was implanted to the skull CSD of dogs, and evaluated for a longer period. While the defects of the negative control group were not filled with new bones, the implant was stabilized to the surrounding bone tissues with fibrous tissues and maintained their shape without any deformation for the whole observation period. This result indicated that this tailor-made implant can be use for CSD of the skull in dogs without any harmful effect.

On CT images, the new bone was observed at the inside of the cylindrical holes and the peripheral implant attaching to the surrounding skull in the TI and fTI groups, which contributed the stronger stability of the implant. In spite of biological degradability of the implant, the volume of implant measured on CT gradually increased after implantation during the experimental period (Nagase *et al.* 1989; Boeree *et al.* 1993; Liuyun *et al.* 2009). In addition, the volume of implant of the fTI group increased significantly more than that of TI group after 2 months of implantation. The measured volume of the implant on CT images does not indicate the actual volume of the implant, and it is very difficult to distinguish between the implant and the regenerated bone on CT images, because CT images are always influenced by partial volume effects in which the margin of the image

makes blur between high and low density area on CT images (Alexander *et al.* 1995). However, gradually increasing volumes in the TI and fTI groups must indicate increases in the regenerated bone within the cylindrical holes and around the implant during the experimental period.

High-quality micro-CT is useful for qualitative and quantitative evaluation of bone density, trabecular bone structure, bone stereology and microarchitecture (Buchman *et al.* 1998; Genant *et al.* 1999; Borah *et al.* 2001). However, when the subject contains the calcium phosphate-based implant, it is difficult to measure the regenerated bone alone, because calcium phosphate and the regenerated bone have similar density on micro-CT images. However, But, it was obvious that more regenerated bones in the fTI group were formed than in the TI group within the hole of implants on the reconstructed micro-CT images in this study.

The combination of fluorochrome staining has been widely used in *in vivo* studies for evaluation of bone healing (Pinholt *et al.* 1990; Pautke *et al.* 2005). Double labeling by fluorochromes has been performed to investigate the mineral apposition rate and bone formation dynamics (van Gaalen *et al.* 2009). In this chapter, bone labeling was performed using oxytetracycline, calcein and alizarin complexone in the early, middle, and later stage of the experimental period,

respectively. In the fTI group, oxytetracycline-stained bone tissues were extensively observed at the regenerated bone, more than in the TI group. bFGF expression on the bone defect was reported to be observed in 2–4 weeks after the implantation (Haque *et al.* 2007). bFGF induces the osteoblastic cell proliferation and new bone formation before 4 weeks after administration (Okazaki *et al.* 1999; Kawaguchi 2005). In this study, oxytetracycline was injected at 2 and 4 weeks of implantation, when bone regeneration was active possibly due to the bFGF effect. And, the results of histological findings, CT and micro CT images showed more regenerated bone tissues in the fTI group than in the TI group. Therefore it may be concluded that the regenerated bone tissues by the effect of bFGF were formed at an early phase of implantation in the fTI group.

Calcein-labeled bone tissues were observed at the regenerated bones and around the Haversian canal located in the inside of oxytetracycline labeled bone tissues. Calcein was injected 6 months of implantation, thus, these findings may indicate that the remodeling was in progress in the regenerated bone tissue at the middle stage of this experiment. Difference between calcein-labeled bone tissues between the TI and fTI groups was not clear. These results indicate that the activity of bFGF of the fTI group did not continue until the middle phase of this study, and

bFGF may be degraded *in situ* or fully released before 6 months of implantation.

Alizarin complexone was administered at the late phase (12 months after the implantation) to avoid minor cytotoxicity, and there seemed no cytotoxic responses (Rahn *et al.* 1972). Alizarin complexone-labeled bone tissues were not clearly observed in all groups. This implied that bone regeneration and remodeling were very slow or almost stopped in this phase.

Fluorochrome labeled bone tissues can be slowly replaced to the new bone which formed after fluorochrome administration by the bone remodeling process. The oxytetracycline-labeled bone tissue was observed clearly at the end of this experiment 12 months after implantation. From the result, it was concluded that the long-term observation using fluorochrome was also available.

Besides the fluorochrome used in this experiment, many kinds of fluorochrome have been used for labeling of the bone tissues (Pautke *et al.* 2005; Pautke *et al.* 2007). Clearer and more specific observation on the variation of regenerated bone in the bone defects would be possible by using the combination of other fluorochromes.

On histology, the area of the regenerated bone within the cylindrical holes in the fTI group was much larger than that in the TI group. This result was consistent to

previous reports on the effects of bone healing promotion by bFGF *in vivo* (Kawaguchi *et al.* 1994; Murakami *et al.* 2003; Oi *et al.* 2009). At 12 months after implantation, almost the half area of the inside of cylindrical holes was filled with fibrous tissues in the fTI group. This was thought to be caused by the fact that bFGF was not incorporated at all the surface of the inside of cylindrical holes. Because cylindrical holes were too narrow to incorporate bFGF using a micropipette, it was not possible to equally incorporate bFGF to all surfaces except the inlet part of cylindrical holes. Therefore, the regenerated bone of the deeper inside of cylindrical holes was not influenced by bFGF. If the incorporation of bFGF onto the whole surface of cylindrical holes would be possible, the increased formation of the regenerated bone would be expected.

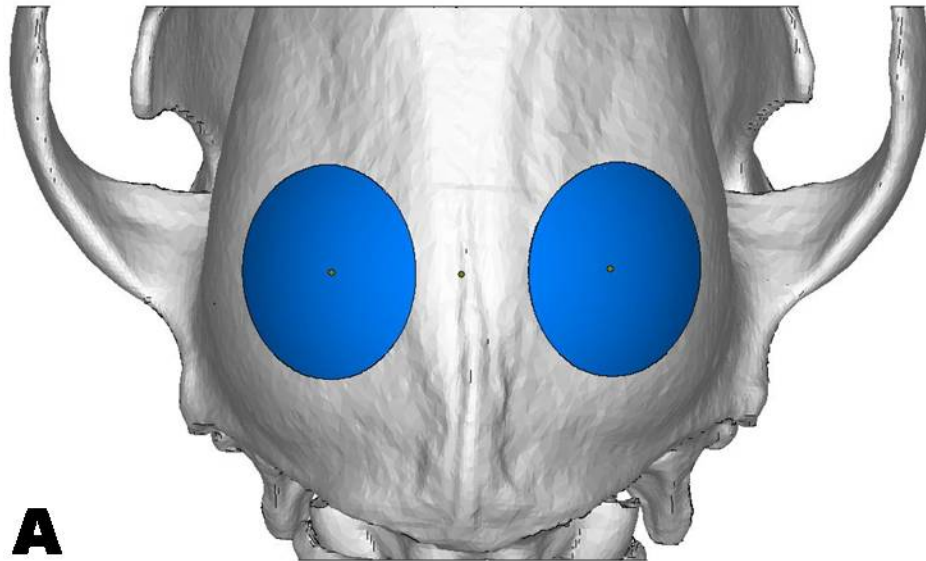
According to the results in Chapter 2, the regenerated bone was mainly formed at the surrounded periosteum. In this chapter, such regenerated bone was observed on CT image at only 1 month of implantation in the fTI group. However, such regenerated bone was disappeared at 2 months of implantation and was also not found on histological findings. The result showed that the bone lining cell of the periosteum proliferated by bFGF might be resorbed by the remodeling process according to the longer experimental period (Suda. 2007).

It is well known that the mechanical strength of calcium phosphate implants is lower than that of the normal bone (Hollister *et al.* 2005). The change in compression strength of calcium phosphate implants is well known in *in vitro* studies (Fukase *et al.* 1990; Frankenburg *et al.* 1998; He *et al.* 2008). However, it is difficult to measure the compression strength of the tailor-made implant only *in vivo* because of their structural characteristics. Therefore, in this chapter, I evaluated the bending strength of the tailor-made implant and surrounding bone tissues. However, there was no difference in bending strength among the groups. This result may indicate the tailor-made implant did not provide mechanical strength to the bone defects at least in one year after implantation.

In the CSD model of the skull of dogs, the implantation of tailor-made implants did not contribute to the maintenance of loading strength in the bone defects. It may be necessary to observe for a longer period whether this method will obtain the higher strength of the tailor-made implant in this model. As far as in the period in this study, the implant maintained the shape and certain strength of the implant without any harmful effect. Therefore, it may be concluded that the tailor-made implant was proper as the implant for CSD of the skull in dogs. Additionally, when bFGF was incorporated to the tailor-made implant, the bone healing may be promoted.

**Table. 3-1** The protocol and fluoroscopic condition for bone staining

Fluorochrome	Injection timing	Dosage	Labeling	Excitation wavelength (nm)	Emission wavelength (nm)	Filter set
Doxycycline	2 times at 2 weeks 2 times at 4 weeks	20mg/kg	Blue	390-425	520-560	# 18
Calcein	2 times every 2 weeks at 6 months	20mg/kg	Green	494	517	# 10
Alizarin complexone	2 times every 2 weeks at 12 months	20mg/kg	Red	530-580	624-645	# 20



**A**



**B**

**Fig. 3-1** (A) The design of the tailor-made implant. (B) Fabricated tailor-made implant with 6 cylindrical holes

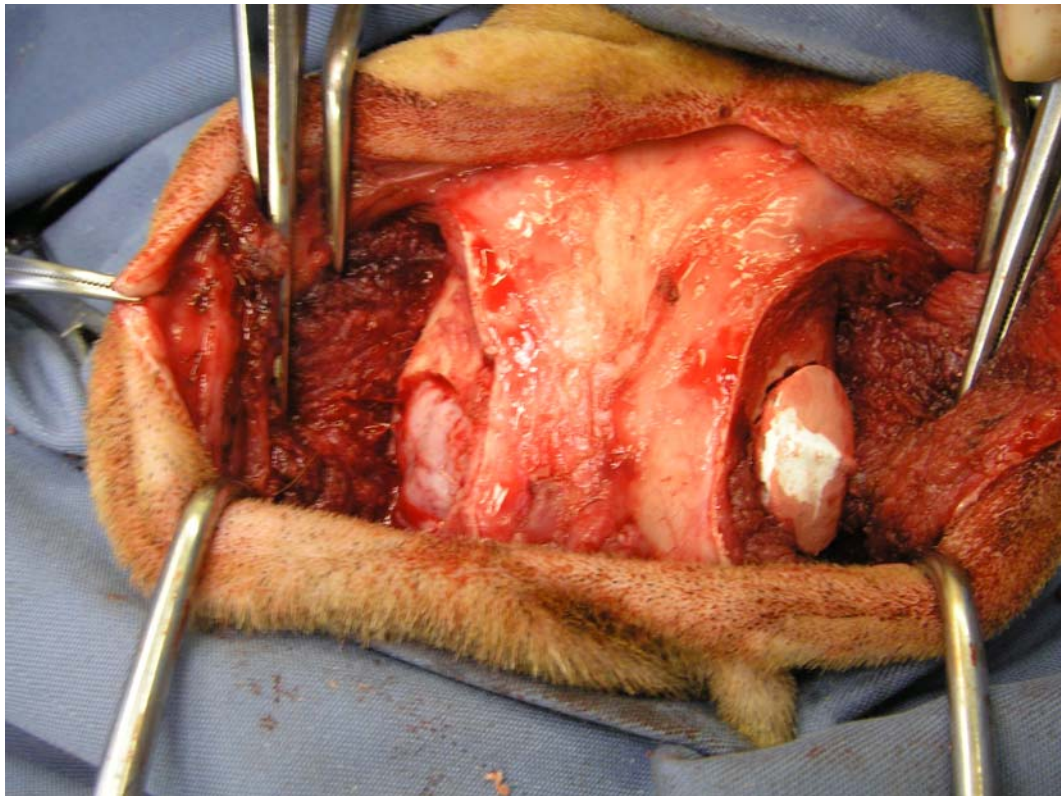


**Fig. 3-2** Two bone defects with 20mm in diameter were created on the bilateral temporalis bone.

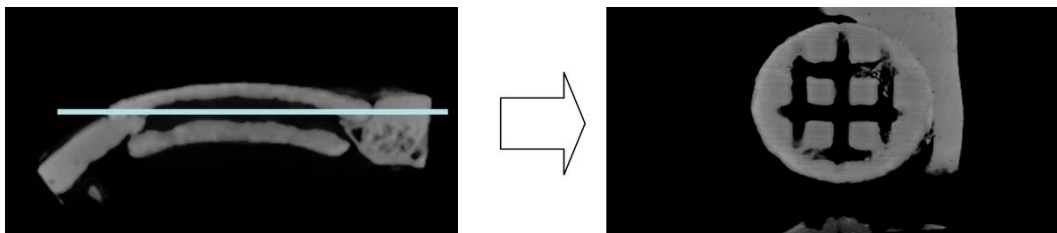


**Fig. 3-3** The section was scanned along z-axis and the obtained images were reconstructed along y-axis using micro-CT analysis program to observe the regenerated bone within the cylindrical holes.

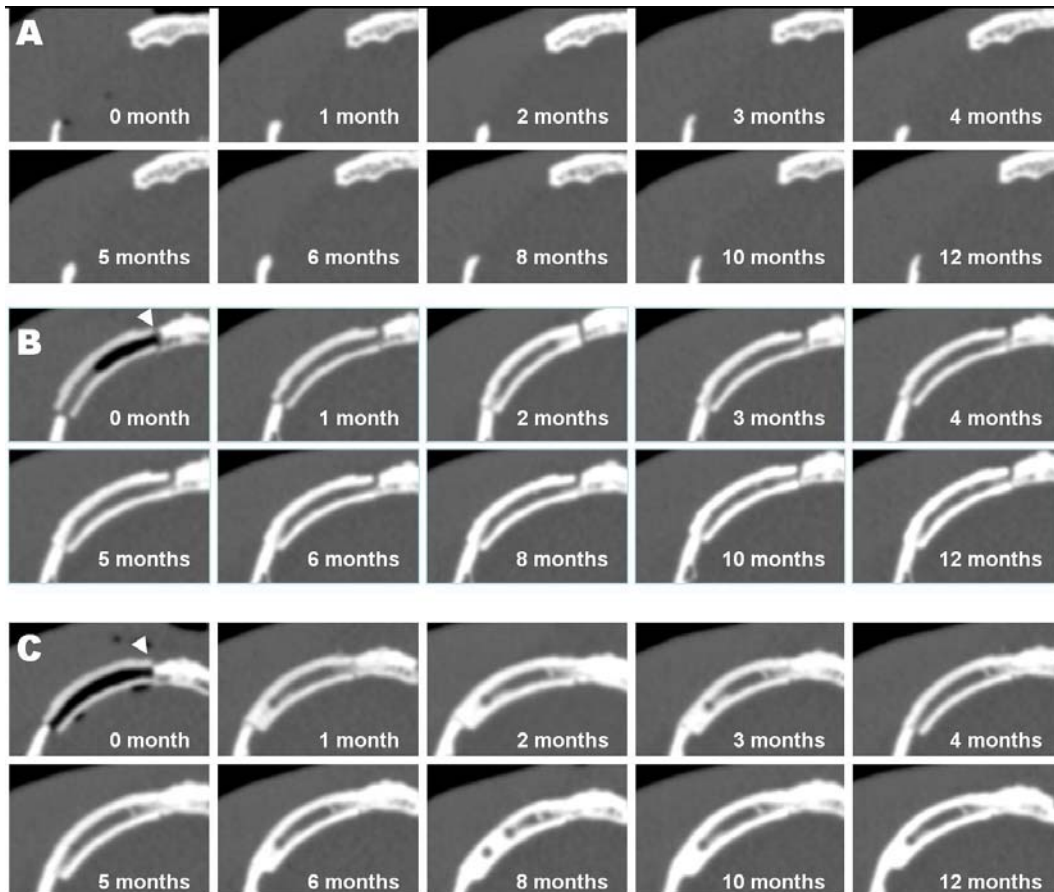


**Fig. 3-4** CT images of each group. In the negative control group, new bone formation was minimal and the defect was open during the whole experimental period (A). In the TI group, the gap (white arrow head) between the implant and the skull was filled with mineralized tissues (B), and in the fTI group, the gap and the cylindrical holes were filled with more mineralized tissues (C).

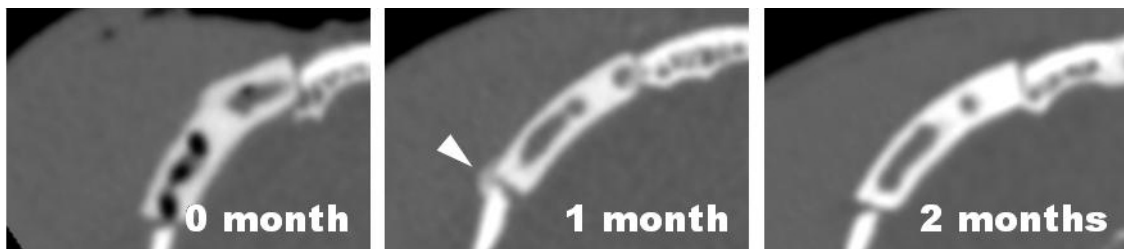


**Fig. 3-5** The regenerated bone on the surrounding periosteum (white arrow head) was observed at 1 month of implantation in the fTI group, but disappeared at 2 months of implantation.

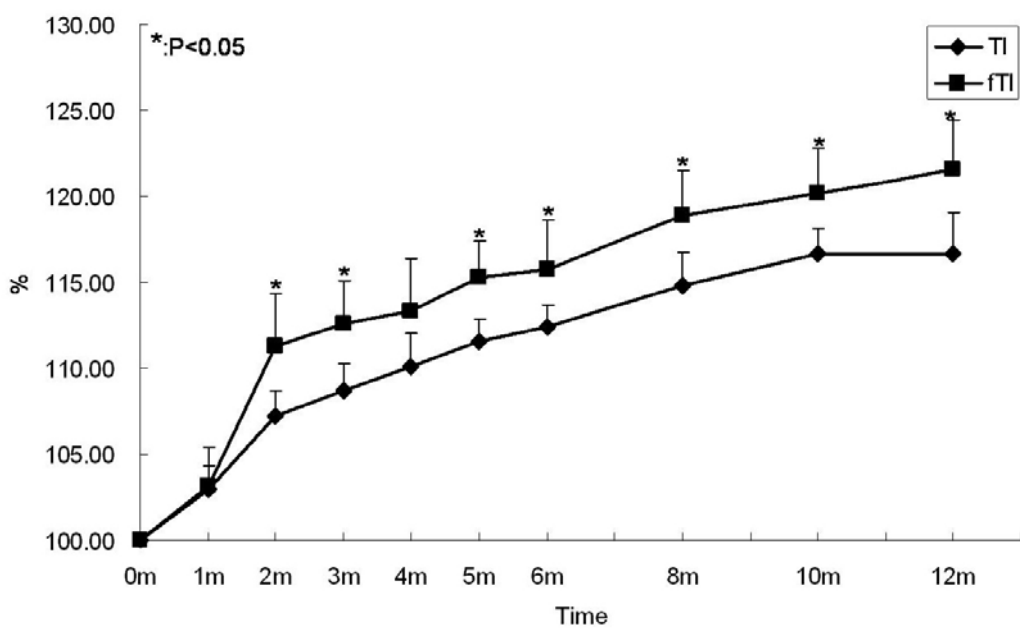


**Fig. 3-6** The changes in the 3 dimensional volume of implants on CT images. The volume of the implant was gradually increased, and that of the fTI group was significantly higher than that of the TI group after 2months of implantation (P<0.05).

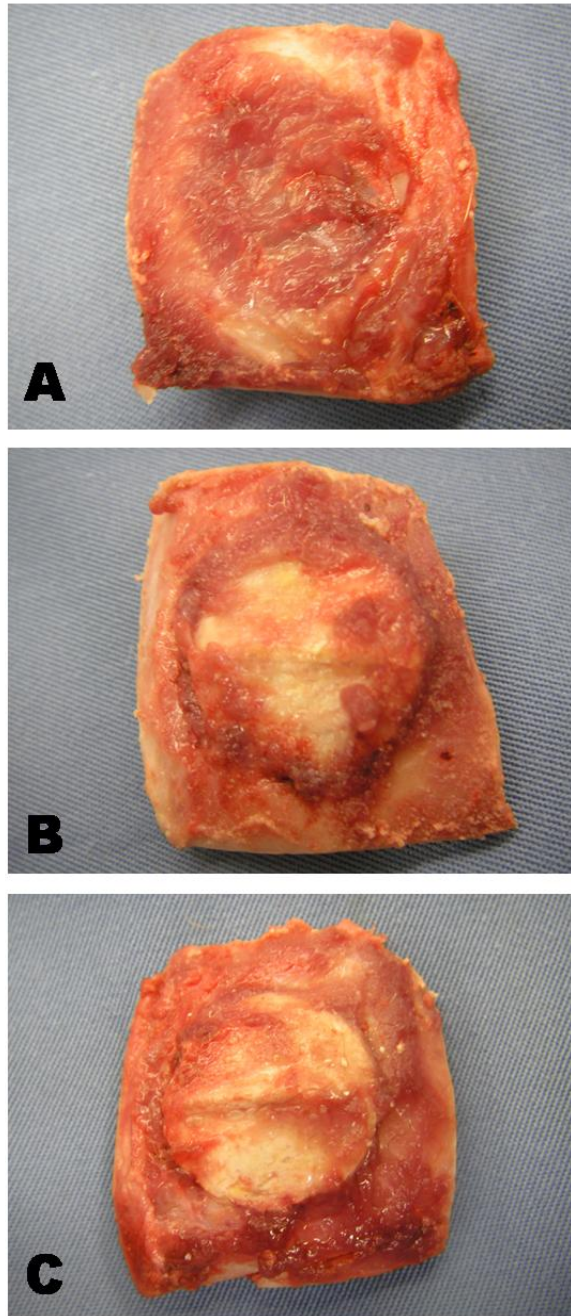


**Fig. 3-7** Gross appearance of excised bone tissues. The bone defects were filled with the muscle and the durameter in the negative control group (A), while the implant was firmly attached to the skull in the TI (B) and fTI (C) groups.

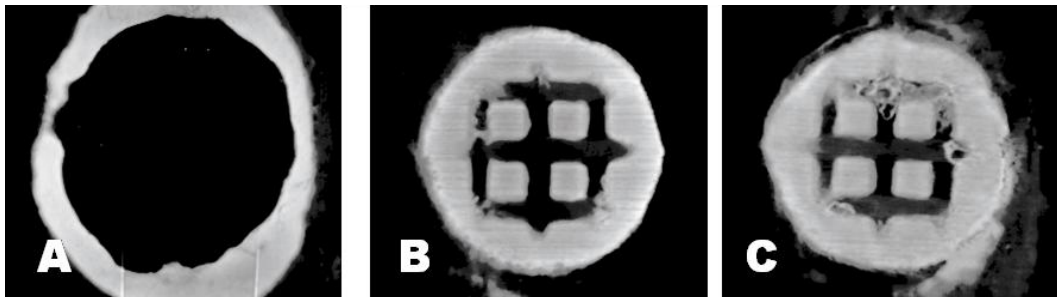


**Fig. 3-8** The micro-CT images of the negative control group (A), TI group (B) and fTI group (C). Small amount of the mineralized tissues existed within the cylindrical holes in the TI group, while more mineralized tissues were observed in the fTI group.

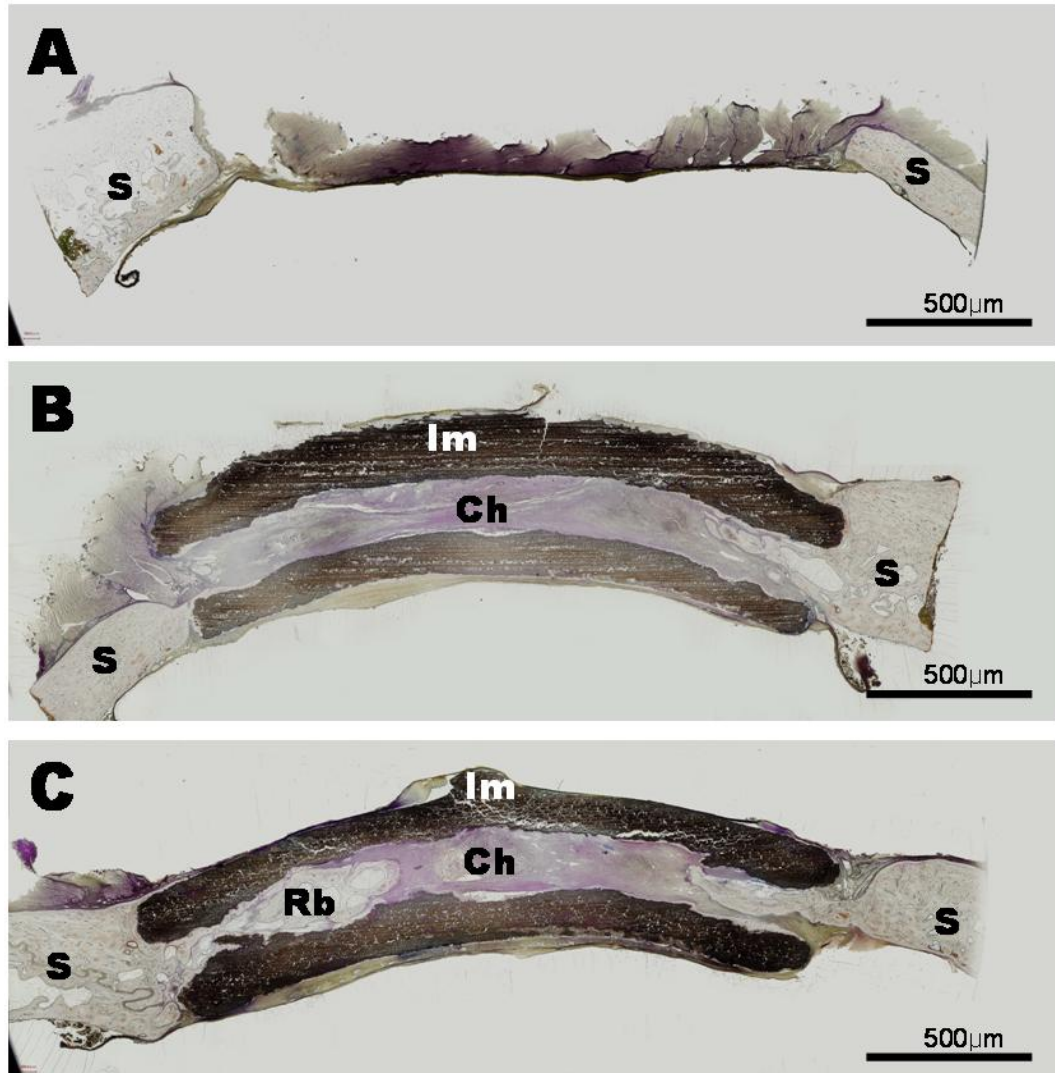


**Fig. 3-9** The typical histological findings of the implant and surrounding tissues of each group. The bone defects were empty without any regenerated bones in the negative control group (A). The implant was attached to the skull by the regenerated bone, and a small amount of new bone formation was observed within the cylindrical hole in the TI group (B). In the fTI group, more regenerated bones within the cylindrical hole existed than TI group (C). (S: skull, Im: implant matrix, Ch: cylindrical hole, Rb: regenerated bone)

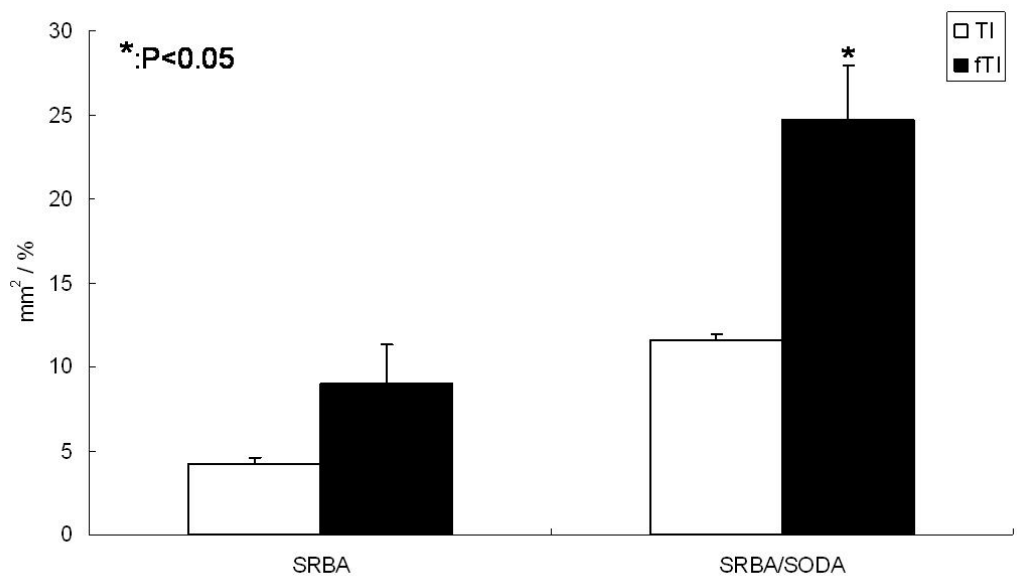


**Fig. 3-10** Measured SRBA and SRBA/SODA of TI and fTI groups.

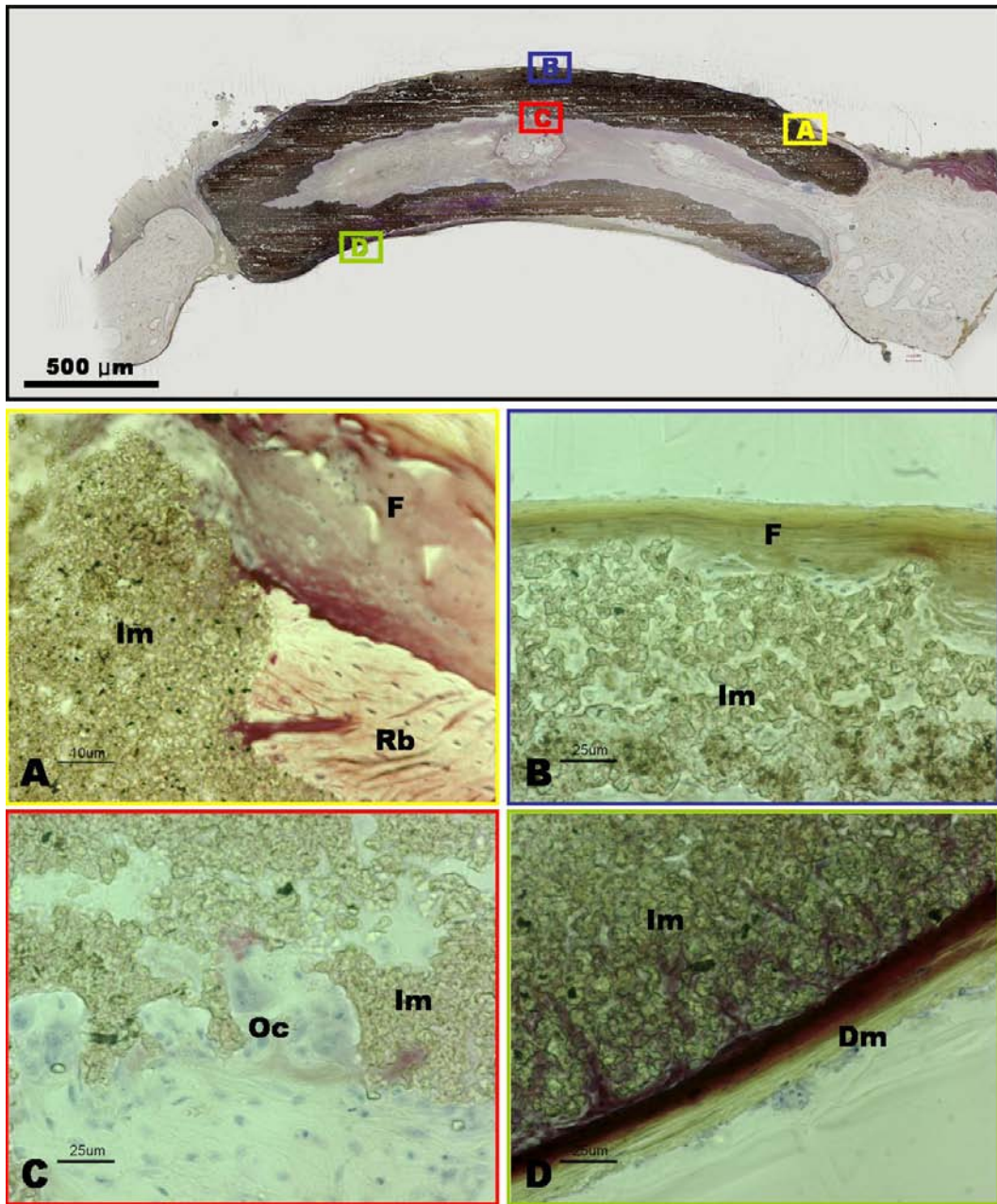


**Fig. 3-11** The surface of the implant matrix in the fTI group. The implant matrix was replaced by the regenerated bone while maintaining the surface shape (A). The outside of the implant maxrix was smooth without matrix resorption and covered with the fibrous tissue and the dura mater, respectively (B, D). The surface of the cylindrical holes was rough, and a lot of the osteoclasts were observed along the surface of the matrix (C). These findings were similar in both the TI and fTI groups. (Im: implant matrix, F: fibrous tissue, Dm: dura mater, Rb: regenerated bone, Oc: osteoclast)

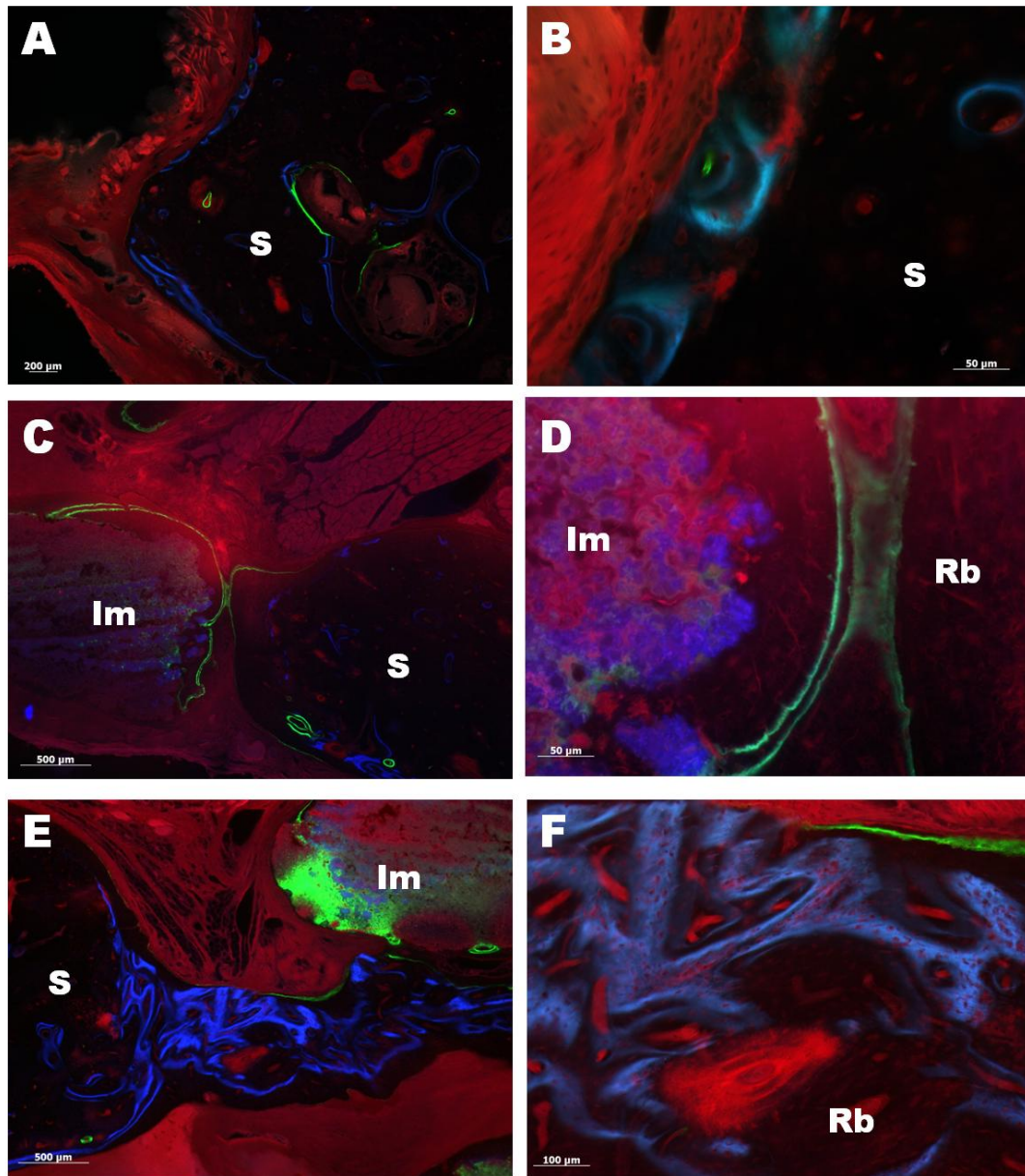


**Fig. 3-12** Three types of fluorochrome were labeled to the bone tissues in the negative control (A, B), TI (C, D) and fTI (E, F) groups. The blue label indicates the oxytetracycline-labeled bone tissues which were formed at the time of 2 and 4 months after implantation. Green label indicates calcein-labeled one which was formed at 6 months after implantation. Red label indicates alizarine complexone-labeled one which was formed at 12 months after implantation. (Im: implant matrix, S: skull, Rb: regenerated bone)

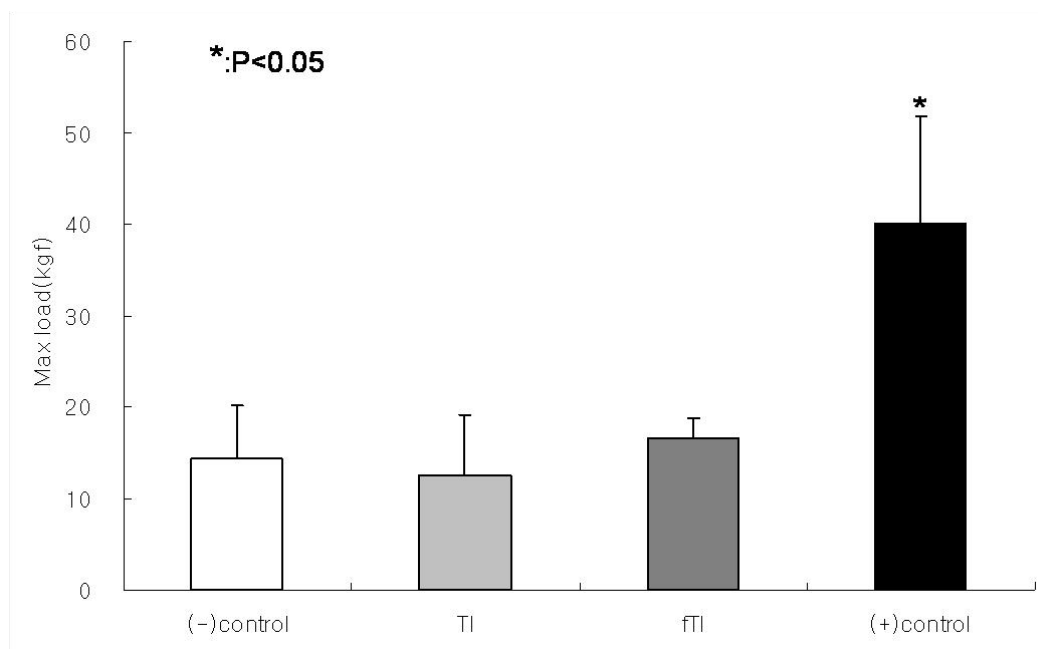


**Fig. 3-13** Mean bending strength (at maximum loading). The strength of the normal skull was significantly higher than that of 3 experimental groups, and there was no significant difference among experimental groups.

**Chapter 4. Effect of implantation of bFGF-  
incorporated tailor-made implants on the repair of  
radial segmental defects in dogs**

## **Introduction**

There are two types of the bone formation process; intramembraneous ossification, and endochondral ossification. The intramembraneous ossification is regulated by the the periosteal osteogenic layer, and the process produces flat bones such as the mandible and the skull. The endochondral ossification is the process associated with fetal bone development, and is observed in the synthesis of the bone on a mineralized cartilage scaffold. This is the type of bone formation found in the development of load-bearing long bones such as vertebrae and long bones of limbs (Shapiro 2008).

The segmental bone defects of a limb were often experimentally used for the evaluation of osteoconductive scaffolds (Holmes *et al.* 1987; Bruder *et al.* 1998; Segal *et al.* 2009). Implants on load-bearing sites should tolerate loading and be optimized to the mechanical environment. A few load-bearing scaffolds have been described in the literature, most of which were the studies on tissue engineered bone regeneration with osteoinductive factors and were conducted at non-loading sites or defects stabilized with stress-shielding devices such as bone plates or external fixation (Einhorn *et al.* 1984; Lieberman *et al.* 1999; Xu *et al.* 2005).

The implant made of calcium phosphate has been used for bone defect in

clinical practices (Fukase *et al.* 1990; Nair *et al.* 2009). However, the calcium phosphate implants are generally very fragile because of its porous structure. Thus, despite of their favorable biological properties, the poor mechanical properties of these ceramic materials have severely hindered their clinical applications (Ducheyne 1987; Yaszemski *et al.* 1996).

bFGF is expressed in the epiphyseal growth plate (Sullivan *et al.* 1985; Twal *et al.* 1994). bFGF plays an important role in endochondral ossification as a mitogen for proliferative zone cells and as an angiogenic factor for vascularization of hypertrophic zone lacunae (Eppley *et al.* 1988; Presta *et al.* 1988). Some investigations have shown that bFGF has a proliferative effect on bone formation in appendicular bones *in vivo* (Nakamura *et al.* 1998; Okazaki *et al.* 1999). Incorporation of bFGF to the implant increases bone growth, stimulates osteoblastic activity, directly stimulates the early proliferative repair stage, and modulates the inflammatory response (Thoren *et al.* 1993; Komaki *et al.* 2006).

The tailor-made implant was used in non-load-bearing sites such as the skull up to the present (Igawa *et al.* 2006; Choi *et al.* 2009). However, according to the results in the previous chapters, the effectiveness in the load-bearing sites should also be evaluated for the clinical application in the future. In this chapter, I

investigate the possibility of the tailor-made implant for the radial segmental defect in dogs and evaluate its promotive effect of the bFGF-incorporated implant on bone repair.

## **Materials & Methods**

### *Preparation of implants*

**Implant fabrication:** Implant fabrication was the same as in Chapter 2. Reconstruction data of the radial shaft with 20mm in length on 3D image were obtained. The reconstructed area of the radial shaft was 45mm distal from the radial tuberosity of the elbow joint. The bone marrow cavity was also reconstructed via CT data, and was expected to have the same function as the cylindrical holes. Using these data, the final TI design was determined and fabricated using an ink-jet printer as in Chapter 2 (Fig. 4-1).

**Trehalose coating:** Trehalose coating process was the same as in Chapter 3.

**bFGF infiltration:** For bFGF-incorporated tailor-made implant with trehalose coating (fTI group), 10  $\mu$ l of bFGF solution was dropped around the inlet of the proximal and distal implant with a micropipette at a total dose of 100  $\mu$ g bFGF per implant, and the implant was dried for 10 minutes at room temperature. Deionized water instead of bFGF was used similarly to TI with trehalose coating (TI group).

### *Experimental animals*

Three female beagle dogs with the body weight from 8.7 kg to 11.7 kg (mean

9.7kg) and the age from 1 year to 2 years were purchased from Nosan Corporation.

Physical condition was examined as described in Chapter 3.

All the experimental procedures using dogs were conducted under the Guidelines of the Animal Care Committee of the Graduate School of Agricultural and Life Sciences, the University of Tokyo.

### ***Surgical procedures***

The anesthetic procedures and aseptical preparation were the same as in Chapter 3. The cranial skin and subcutaneous tissues were incised from the elbow to just above the carpus. The deep antebrachial fascia was incised between the extensor carpi radialis muscle and the flexor carpi radialis muscle to expose the shaft of radius. The supinator muscle was bluntly dissected from the periosteum for the plate application.

An eight-hole lengthening bone plate, in which metal bar was used to immobilize fractured segments with central solid section without screw holes to span the defect, was placed on the cranial surface of the shaft of radius. Two drill holes with 2.0 mm in diameter at the proximal and distal portions were drilled through the two cortices using a surgical drill (Stryker Instruments, Kalamazoo,

USA), and tapped with a 2.7 mm tap. The plate was then removed and 20 mm segmental bone defect, known as critical size defect in radius of dogs, was created at 45mm distally from the radial tuberosity (Hollinger *et al.* 1990; Johnson *et al.* 1996). Deionized water-incorporated implant was implanted in the left radius (TI group), and bFGF-incorporated implant was implanted in the right radius (fTI group). The plate was placed on the same position, and 6 other screw holes were created and tapped at the proximal and distal portions. The cortical screw with 2.7mm in diameter was inserted to each screw hole to stabilize the radial defect (each group n=3; Fig. 4-2). Closure of the surgical wound was similar to that in Chapter 2.

The Robert John's bandage was applied to bilateral forelimbs for 7 days after surgery, and an antibiotic (cefazolin, 20 mg/kg subcutaneously, twice daily) and an analgesic (buprenorphine, 15 µg/kg intramuscularly, twice daily) were injected for 3 days postoperatively.

### ***Radiography***

Radiography was conducted immediately after the surgery and at 2 and 4 weeks of implantation. The lateral radiographs were taken for bilateral forelimbs, and the

callus formation between the radius and the implant was observed.

### ***Gross evaluation***

At 4 weeks of implantation, the dogs were euthanatized with 30 mg/kg thiopental sodium and KCl. The bone plate and the cortical screws were removed, and the implant and surrounding tissues were observed carefully and excised using a sagittal saw.

### ***Histology***

Excised tissues were fixed with 10% neutered formalin (WAKO) for 5 days. Tissues were decalcified with plank-rychlo decalcifying solution (WAKO) for 1-2 month. The decalcifying solution was changed every 3-4 days. Decalcified tissues were trimmed parallel to the long axis, and embedded in paraffin. The tissue block was cut into 7- $\mu$ m thick sections, and stained with Masson's trichrome after deparaffinization. The stained sections were examined under a light microscope and measured the area of regenerated bone from the periosteum and constitution of regenerated tissues such as regenerated bones, blood vessels and fibrous tissues in cylindrical hole using image J software (US National Institutes of Health).

### *Statistical analysis*

The mean values and SD of the area of regenerated bone was calculated, and student t-test was performed using spreadsheet program (Excel, Microsoft Coporation). P-value less than 0.05 was considered to be statistically significant.

## **Results**

There were no clinically abnormal signs such as pain, inflammation and lameness in dogs receiving the implantation during the whole observation period.

### ***Gross evaluation***

In the TI group, only one implant was firmly united to the radius and surrounding tissues with the callus. The other two implants of the TI group were not united to the radius and had the crack in the implant body. In the fTI group, all implants were firmly united to the radius and surrounding tissues with the callus (Fig. 4-3).

### ***Radiographic findings***

Fig. 4-4 shows radiographic images of each group. In the TI group, all the implants were slightly rotated at 2 weeks of implantation. The osseous callus was revealed between the distal radius and the implant at 4 weeks of implantation. In the fTI group, all the implants were slightly rotated like that of the TI group. However, the osseous callus was clearly shown between the proximal / distal radius and the implant at 4 weeks of implantation.

### ***Histology***

Fig. 4-5 shows typical histological findings of the implant and the surrounding tissues of each group. The implants of all the groups were slightly dislocated from the implanted site and were surrounded with the fibrous tissues. The regenerated bone tissues were shown at the periosteum adjacent to the implant (Fig. 4-5 A, B). The area of the regenerated bone on the periosteum was  $3.33 \pm 1.92 \text{ mm}^2$  in the TI group and  $9.09 \pm 9.04 \text{ mm}^2$  in the fTI group, respectively. There was no significant difference between the two groups (Fig. 4-6).

The cylindrical hole was fully filled with the fibrous tissues, the regenerated lamellar bones and blood vessels (Fig. 4-5 C, D). Ratios of the regenerated tissues in the cylindrical hole were  $5.0 \pm 4.5 \%$  of the regenerated bones,  $3.5 \pm 0.9 \%$  of the blood vessels and  $93.6 \pm 3.8 \%$  of the fibrous tissues in the TI group. In the fTI group, the regenerated bones occupied  $16.5 \pm 18.9 \%$ , the blood vessels occupied  $5.1 \pm 1.6 \%$  and fibrous tissues occupied  $78.4 \pm 20.4\%$ , respectively. There was no significant difference between the two groups (Fig. 4-7).

## Discussion

Various types of materials have been used as implants for the site with load-bearing, and carriers incorporated with osteoinductive factors have also been used (Komaki *et al.* 2006; Chu *et al.* 2007). Ramay *et al.* reported that the biphasic calcium phosphate implant, composite of hydroxyapatite and  $\beta$ -TCP, should be used for load-bearing bones to enhance the mechanical properties of the scaffold (Ramay *et al.* 2004). In this study, potential usefulness of tailor-made implants incorporating bFGF for the large segmental defect of the long bones was evaluated.

In this study, while the implants of the fTI group were firmly united to the radius, the implants of the TI group had cracks and did not unite to the radius. The crack of the implant is fatal because it may induce pain to patients and lead to instability of the implant. These results may indicate that the implant of the TI group was too weak to bear the load to the defect site although the segmental defect was stabilized by a bone plate. A little load-bearing force may be present at the implant site which induced micro movement of the implant, leading crack formation. On the contrary, in the fTI group, there was no crack and significant dislocation of the implants, leading to the full uniting of the implant to the

surrounding tissues with the hard tissues or callus. bFGF incorporated in the implant could promote the mitosis of various undifferentiated cells and the vascularization (Thomas 1987; Rifkin *et al.* 1989), which may induce an earlier stabilization of the implant. After stabilization, the load to the implant was distributed to the adjacent tissues, leading to prevention of the crack.

bFGF promotes the fracture healing on the appendicular bone through the endochondral ossification process by stimulation of bone remodeling (Nakamura *et al.* 1995). In this study, there was no significant difference in the new bone formation between the two groups. Moreover, the differences in the area of regenerated bones in both groups seemed to be less than the results obtained in Chapter 2. Although the total dose of bFGF was similar to that used in Chapter 2, the effect of bFGF on bone regeneration seemed not enough in this chapter. In this study, the implant had two surfaces (proximal and distal) to the radius, then the volume of bFGF to each surface should be half (50  $\mu\text{g}$  bFGF). Komaki *et al.* investigated the effect of 200  $\mu\text{g}$  bFGF incorporated to the composition of  $\beta$ -TCP and type 1 collagen, and showed that a large amount of bone formation in the tibial defect model (Komaki *et al.* 2006). Nakamura *et al.* reported a single injection of 200  $\mu\text{g}$  bFGF to the tibial fracture site and showed more periosteal callus than that

of the control group (Nakamura *et al.* 1995). Based on these studies, the amount of bFGF in this study may not be enough to promote the regenerated bone formation. If the total amount of bFGF added would be increased, it might be possible to obtain more potent promotion effects of the regenerated bone formation in this bone defect model because the osteoinductive effect of bFGF is dose-dependent *in vivo* (Draenert *et al.* 2009).

In this study, I designed the implant without additional openings other than the cylindrical hole, similar shape and size to the bone marrow cavity. The bone marrow cavity has the endosteum and the mesenchymal stem cells (MSCs) *in vivo*. MSCs possess a high replicative capacity and are able to form bones and other tissues (Haynesworth *et al.* 1992; Bruder *et al.* 1997; Jaiswal *et al.* 1997). When MSCs combined with a adequate carrier, it can lead to osteogenesis *in vivo* (Petite *et al.* 2000; Fialkov *et al.* 2003). I expected that the cylindrical holes of the implants connected to the bone marrow cavity of the radius would be quite effective to induce a large amount of the regenerated bone by osteogenic differentiation of MSCs and the endosteum proliferation. However, histological findings in the cylindrical hole in all groups did not show such a large amount of bone formation. This may be due to loss of connection to the bone marrow cavity

of the radius due to dislocation of the implant at an early phase of implantation (2 weeks).

In conclusion, the tailor-made implant alone was not efficient to the load-bearing site because of its mechanical properties. These problems may be solved through improvement of the implant mechanical strength or shape of the implant. If a higher dose of bFGF was incorporated to the implant, it may be possible to obtain a good bone even repair in the load-bearing site as in the fTI group.

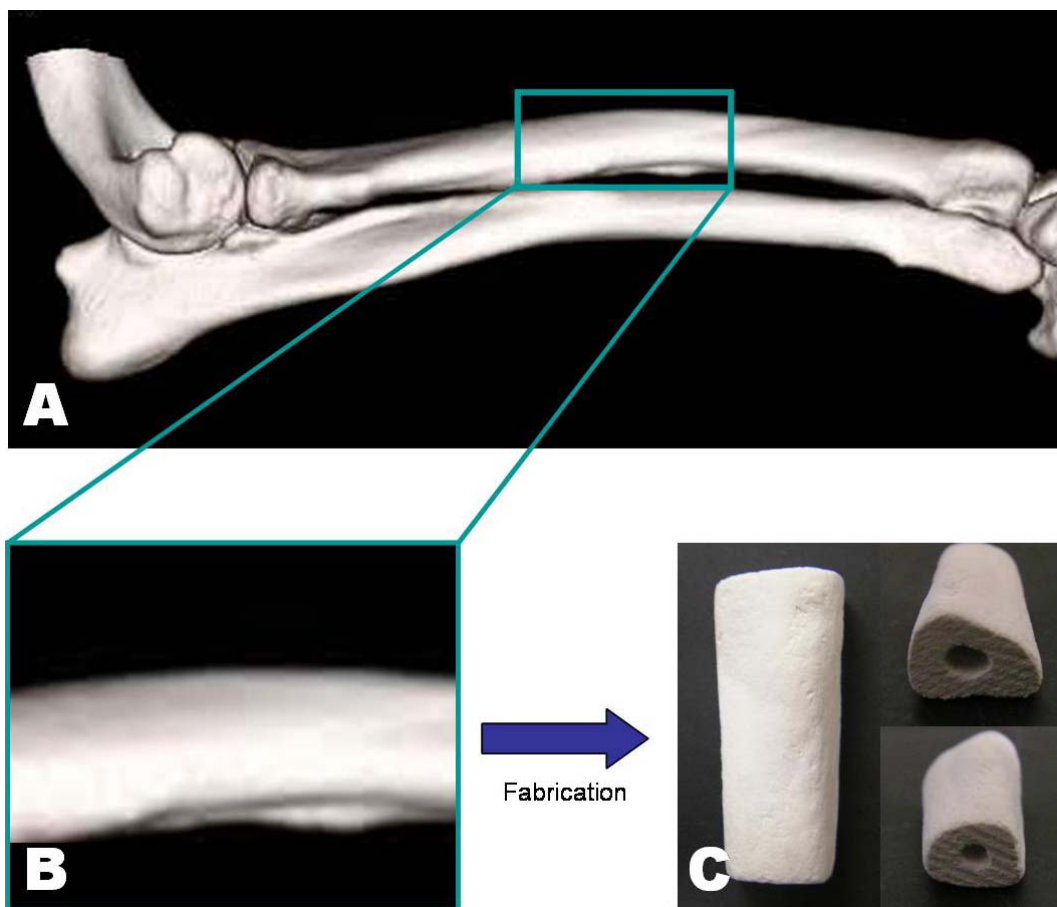


**Fig. 4-1** Fabrication of the tailor-made implant for the radius. The implant was designed for the shaft of radius. The implant had the same structure as the radius and the bone marrow cavity of the implant was used as the function of the cylindrical holes as in the implant for the skull.

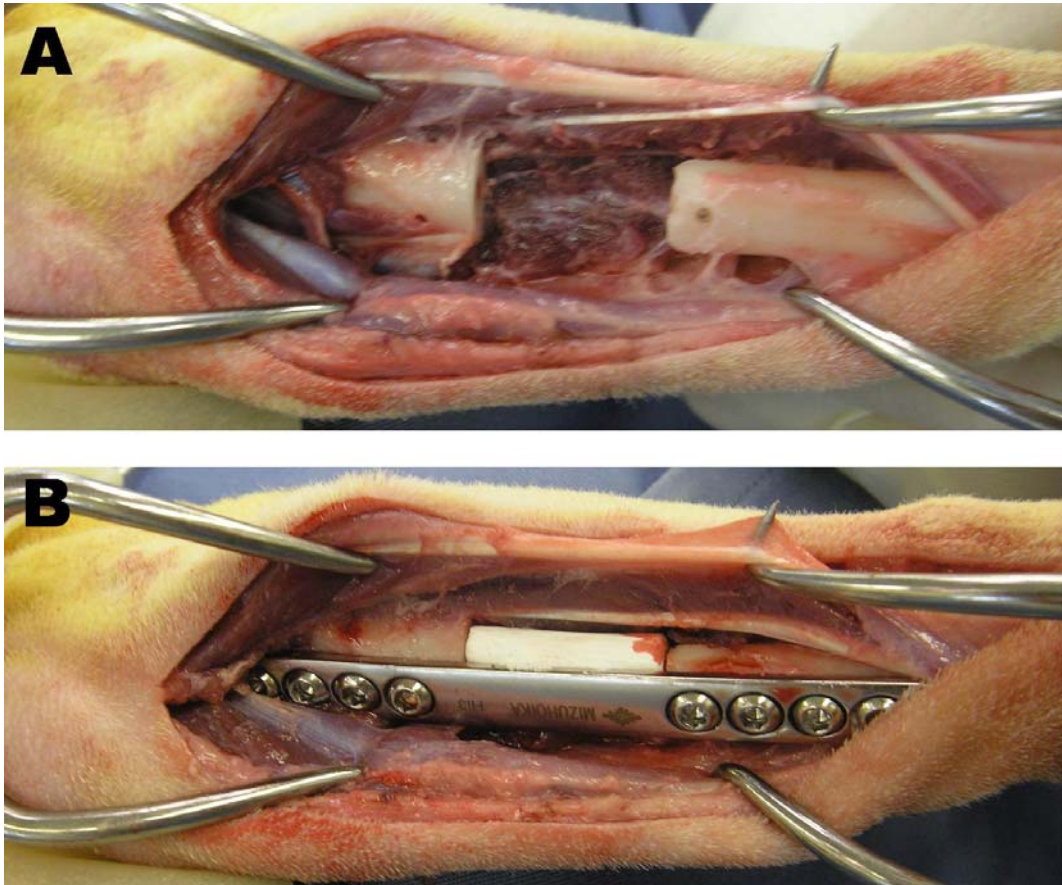


**Fig. 4-2** The picture of radial segmental defect with 20mm in length and 45mm distally from the radial tuberosity (A). Each implant was implanted to the bone defect and the defect was stabilized with a 8-hole lengthening plate (B).

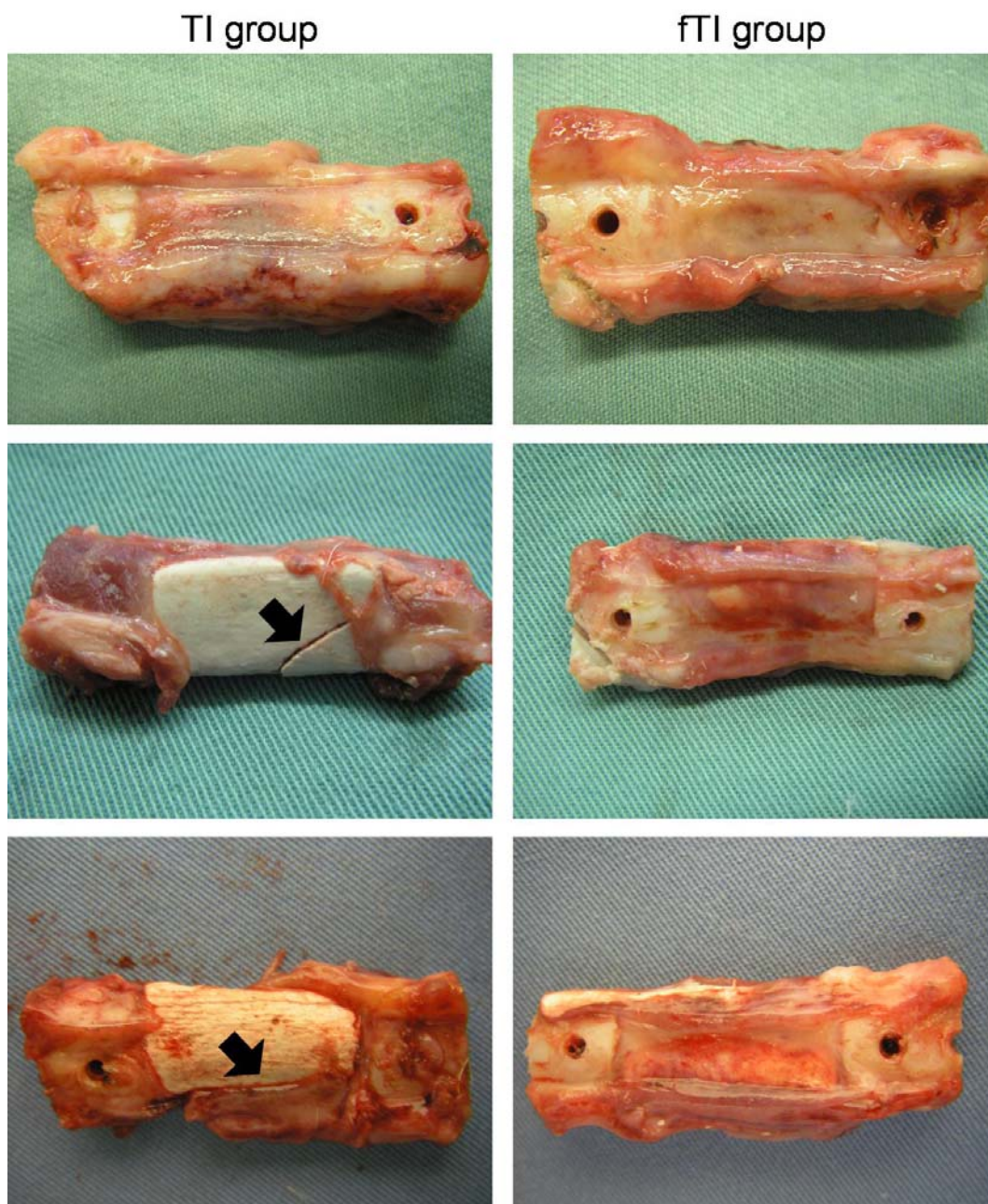


**Fig. 4-3** Gross appearance of excised bone tissues. One implant of the TI group was united to the radius and surrounding tissues with the callus (left top). Two other implants of the TI group were not united to the radius and had the crack in the implant body (black arrows; left middle and bottom). All implants of the fTI group were firmly united to the radius and surrounding tissues with the callus (right).



**Fig. 4-4** Radiographic images of each group. The implants of all groups were slightly dislocated at 2 weeks of implantation. The osseous callus (white arrow head) was observed between the distal radius and the implant in the TI group (A), and the proximal / distal radius and the implant in the fTI group (B) at 4 weeks of implantation.

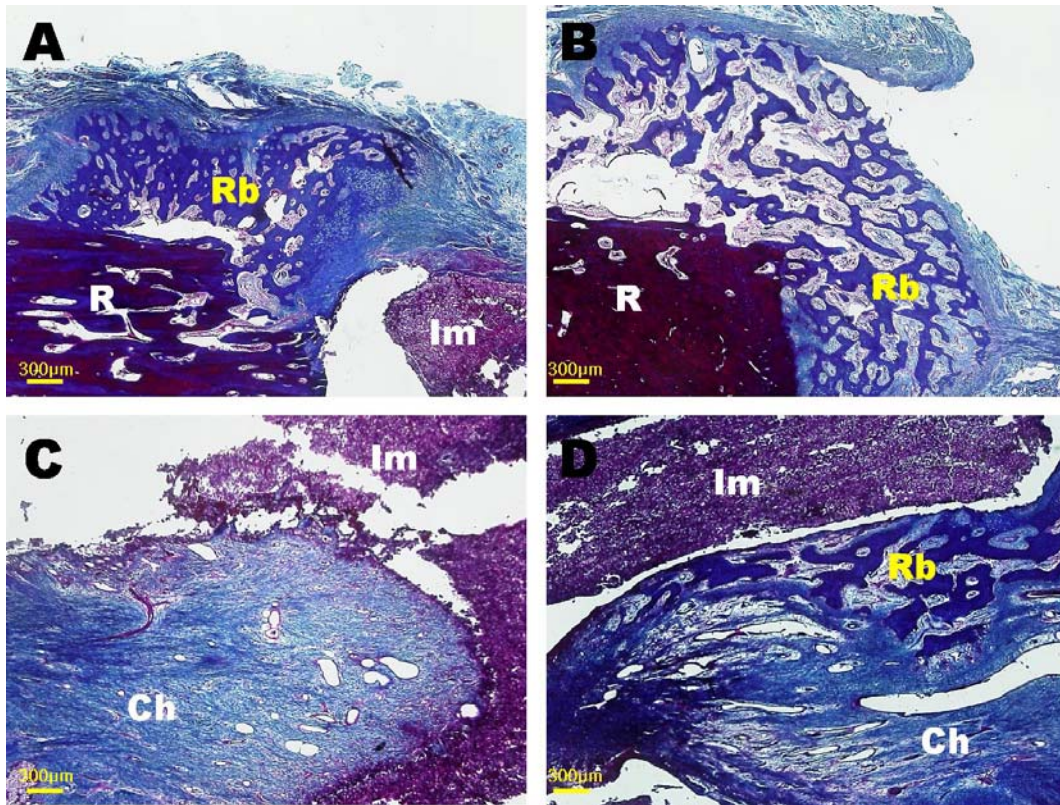


**Fig. 4-5** The typical histological findings of the TI (A,C) and fTI (B,D) groups. A larger amount of regenerated bone in the fTI group (B) was observed on the periosteum adjacent to the implant than in the TI group (A). The cylindrical hole was filled with the fibrous tissues and few blood vessels in the TI group (C). In the fTI group, the fibrous tissues and the blood vessels filled most of the cylindrical hole and the regenerated bone was formed at the surface of cylindrical hole (D). (R: radius, Rb: regenerated bone, Im: implant matrix, Ch: cylindrical hole)

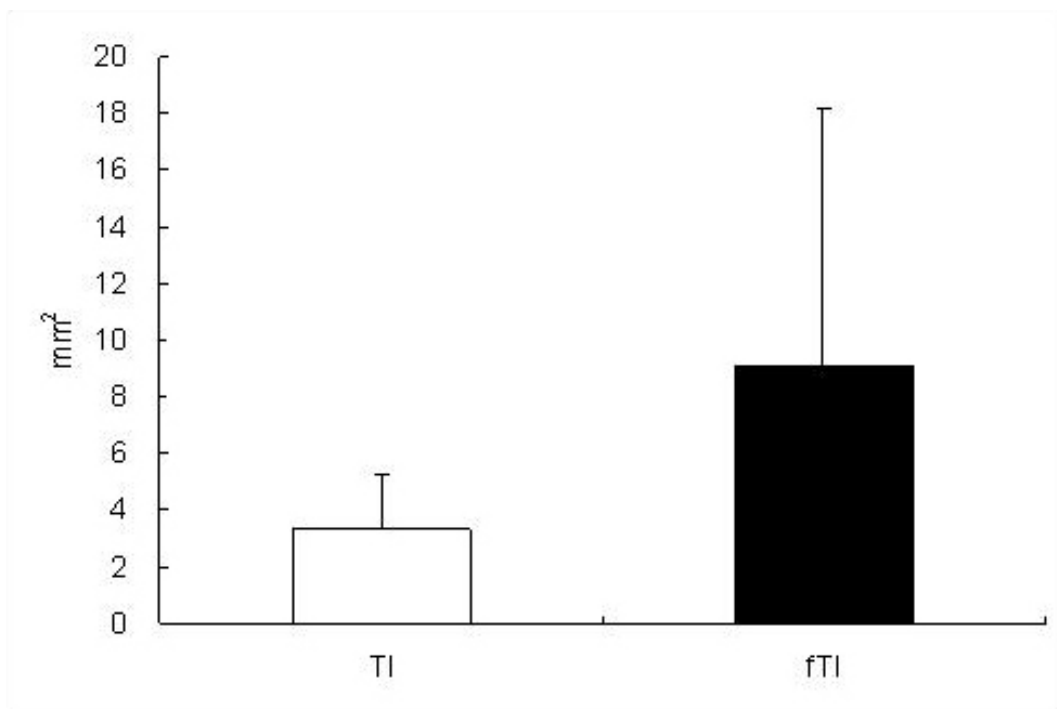


**Fig. 4-6** The area of regenerated bone on the periosteum in each group. Although the area of the fTI groups was twice higher than that of the TI group, there was no significant difference between the two groups.

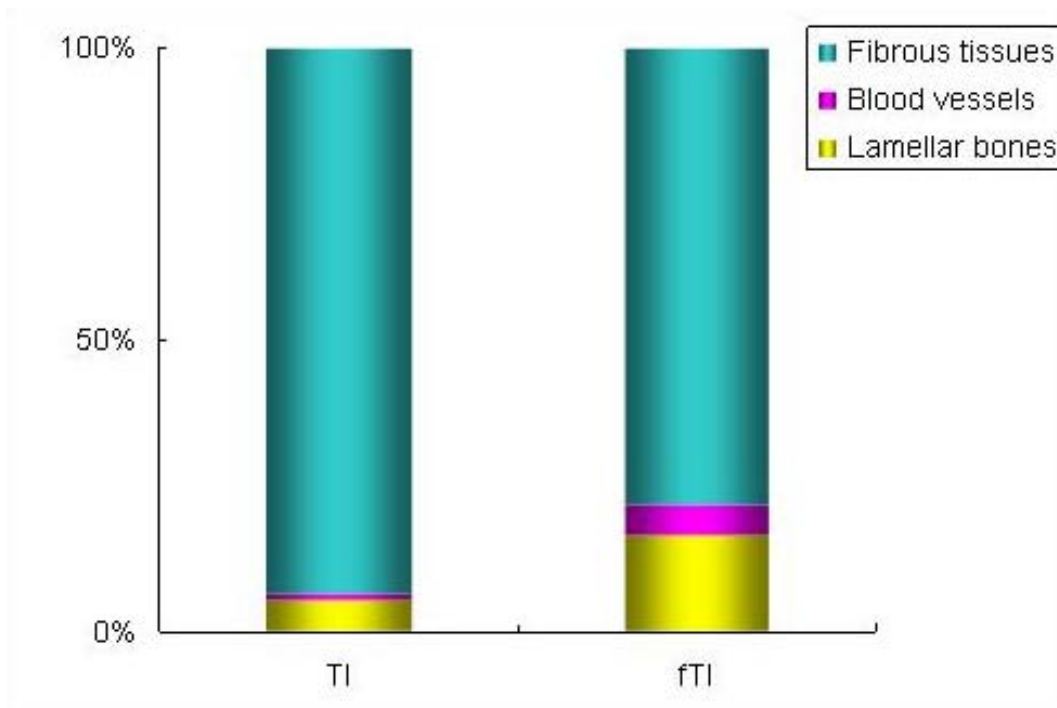


**Fig. 4-7** The constitution of regenerated tissues in the cylindrical hole. The ratios of the lamellar bone of the fTI group was 3 times higher than that of the TI group. And that of the blood vessel of the fTI group was 1.5 times higher than that of the TI group. However, there were no significant differences.

## Conclusion

Bone graft was often used to treat the large bone defect due to trauma, cancers and congenital skeletal deformity. Recently, various artificial bones were developed, among which, calcium phosphate most widely has been used in the clinical practice.

The group of the author has established a tailor-made artificial bone made of  $\alpha$ -TCP fabricated by a 3D ink-jet printer by rapid prototyping techniques. They have shapes well matching to the original bone defect and can be easily implanted to the defect site. This tailor-made implant can be freely designed in its internal structure such as the cylindrical hole, which can facilitate bone ingrowth.

These artificial bones, however, show only osteoconductive function. If osteoinductive agents such as BMP and bFGF would be incorporated to them, more new bone formation at an earlier phase could be expected.

One problem when incorporating these agents to the artificial bone is absorption of these agents to the calcium phosphate, which may be the cause of delayed release of these agents. In this thesis, the clinical usefulness of bFGF-incorporated tailor-made artificial bones for large bone defects was investigated.

In Chapter 1, I investigated the effect of trehalose coating and bFGF on the

proliferation of osteoblastic cells and the mechanical strengths of the implant *in vitro*. When the bFGF-incorporated implant with trehalose coating was inserted in the culture of mouse osteoblast cells, cell number significantly increased when compared to bFGF-incorporated, trehalose non-coated implant. In addition, the mechanical strength of the implant was increased by trehalose coating.

In Chapter 2, I investigated the bone regenerative effects *in vivo* and the optimal dose of bFGF incorporated with the tailor-made implant for the skull defects of dogs. bFGF at various doses was incorporated to the implant with or without trehalose coating, and the implant was implanted to the bone defect of 11mm in diameter of the skull in dogs. According to the data of CT, micro-CT and on histology, incorporation of 100  $\mu$ g dose of bFGF is optimal to promote more bone regeneration. However, there was no significant difference in bone regeneration between implants with and without trehalose coating.

In Chapter 3, I investigated the long-term effect of the bFGF-incorporated tailor-made implant with trehalose-coating on critical size bone defect of the skull of dogs. The bone defect of 20 mm in diameter was created in the skull, and the implant with or without bFGF was implanted. After 12 months of implantation, the implant of two groups was united to the skull without any displacement or

deformity of the implant, and the implant matrix was resorbed by regenerated bone tissues. In addition, the regenerated bone tissues were much more by implantation of the implant with bFGF. According to the data by bone staining and CT, new bone formation was more active at an earlier phase after implantation, probably due to the effect of bFGF. However, mechanical strength at the defect was not improved by the implantation.

In Chapter 4, the segmental defect of load-bearing bones of dogs was created in the radius and this implant was implanted to investigate the usefulness for load-bearing sites. After 4 weeks of implantation, the implants without bFGF showed crack and did not unite to the radius. On the contrary, all the implants with bFGF were united to the radius and surrounded tissues by the callus. These results may indicate that the tailor-made implant alone was not efficient to the load-bearing site because the mechanical strength of the implant was not enough to bear the loading force of the radius. If a higher dose of bFGF was incorporated to the implant, it may be possible to be applied for the load-bearing site.

In conclusion, this bFGF-incorporated tailor-made implant can induce bone regeneration in the early phase in the various bone defects of dogs. These results strongly encourage the use of this implant for large bone defects in the clinical

practice.

## **Acknowledgment**

I would like to appreciate Professor Nobuo Sasaki (Laboratory of Veterinary Surgery, The University of Tokyo) for his continuous supervision and support. I also sincerely thank Professor Ryohei Nishimura, Associate Professor Manabu Mochizuki for their advice, discussion and encouragement. And I would like to show my gratitude to Professor Ung-il Chung (Division of Tissue Engineering, The University of Tokyo) and Dr. Shigeki Suzuki (NEXT 21, K.K.) for their kind advice and encouragement.

I also thank Dr. Takayuki Nakagawa, Dr. Ryosuke Echigo, Dr. Naoki Fujita and other member of the Laboratory of Veterinary Surgery, The University of Tokyo. And I would like to thank Dr. Kazuyo Igawa (Division of Tissue Engineering, The University of Tokyo) and Mr. Akimitsu Miyazaki (NEXT 21, K.K.) for their cordial support.

Finally, I am truly thankful for the continuous support of my parents, brother and sister.

## References

- Alam, S., Ueki, K., Marukawa, K., Ohara, T., Hase, T., Takazakura, D. and Nakagawa, K. (2007). Expression of bone morphogenetic protein 2 and fibroblast growth factor 2 during bone regeneration using different implant materials as an onlay bone graft in rabbit mandibles. *Oral Surg Oral Med Oral Pathol Oral Radiol Endod* 103(1): 16-26.
- Alexander, E., 3rd, Kooy, H. M., van Herk, M., Schwartz, M., Barnes, P. D., Tarbell, N., Mulkern, R. V., Holupka, E. J. and Loeffler, J. S. (1995). Magnetic resonance image-directed stereotactic neurosurgery: use of image fusion with computerized tomography to enhance spatial accuracy. *J Neurosurg* 83(2): 271-6.
- Amstutz, H. C., Johnson, E. E., Finerman, G. A., Meals, R. A., Moreland, J. R., Kim, W. C. and Urist, M. R. (1984). New advances in bone research. *West J Med* 141(1): 71-87.
- Arrington, E. D., Smith, W. J., Chambers, H. G., Bucknell, A. L. and Davino, N. A. (1996). Complications of iliac crest bone graft harvesting. *Clin Orthop Relat Res*(329): 300-9.
- Baba, K., Ishiguro, M., Shimofusa, M., Shibata, H. and Uchinuma, E. (2008). A Case of Craniofacial Reconstruction Using Calcium Phosphate Bone Cement and Titanium Mesh Sheet. *Japanese Journal of Occupational Medicine and*

Traumatology(56): 62-67.

Basilico, C. and Moscatelli, D. (1992). The FGF family of growth factors and oncogenes.  
Adv Cancer Res 59: 115-65.

Boeree, N. R., Dove, J., Cooper, J. J., Knowles, J. and Hastings, G. W. (1993).  
Development of a degradable composite for orthopaedic use: mechanical  
evaluation of an hydroxyapatite-polyhydroxybutyrate composite material.  
Biomaterials 14(10): 793-6.

Borah, B., Gross, G. J., Dufresne, T. E., Smith, T. S., Cockman, M. D., Chmielewski, P. A.,  
Lundy, M. W., Hartke, J. R. and Sod, E. W. (2001). Three-dimensional  
microimaging (MRmicroI and microCT), finite element modeling, and rapid  
prototyping provide unique insights into bone architecture in osteoporosis. Anat  
Rec 265(2): 101-10.

Bruder, S. P., Jaiswal, N. and Haynesworth, S. E. (1997). Growth kinetics, self-renewal,  
and the osteogenic potential of purified human mesenchymal stem cells during  
extensive subcultivation and following cryopreservation. J Cell Biochem 64(2):  
278-94.

Bruder, S. P., Kraus, K. H., Goldberg, V. M. and Kadiyala, S. (1998). The effect of  
implants loaded with autologous mesenchymal stem cells on the healing of  
canine segmental bone defects. J Bone Joint Surg Am 80(7): 985-96.

- Buchman, S. R., Sherick, D. G., Goulet, R. W. and Goldstein, S. A. (1998). Use of microcomputed tomography scanning as a new technique for the evaluation of membranous bone. *J Craniofac Surg* 9(1): 48-54.
- Canalis, E., Economides, A. N. and Gazzerro, E. (2003). Bone morphogenetic proteins, their antagonists, and the skeleton. *Endocr Rev* 24(2): 218-35.
- Cao, B., Xu, Z. S., Xiao, D. M., Lin, B. W., Lu, X. H. and Li, R. (2009). [Biocompatibility of polylactic-co-glycolic acid for culturing bFGF gene-transfected bone marrow stromal cells and application of the cell complex for repairing rabbit cartilage defect]. *Nan Fang Yi Ke Da Xue Xue Bao* 29(6): 1123-6.
- Chen, Q. and Haddad, G. G. (2004). Role of trehalose phosphate synthase and trehalose during hypoxia: from flies to mammals. *J Exp Biol* 207(Pt 18): 3125-9.
- Cheung, C. (2005). The future of bone healing. *Clin Podiatr Med Surg* 22(4): 631-41 viii.
- Choi, S. J., Lee, J. I., Igawa, K., Sugimori, O., Suzuki, S., Mochizuki, M., Nishimura, R., Chung, U. I. and Sasaki, N. (2009). Bone regeneration within a tailor-made tricalcium phosphate bone implant with both horizontal and vertical cylindrical holes transplanted into the skull of dogs. *J Artif Organs* 12(4): 274-277.
- Chu, T. M., Warden, S. J., Turner, C. H. and Stewart, R. L. (2007). Segmental bone

regeneration using a load-bearing biodegradable carrier of bone morphogenetic protein-2. *Biomaterials* 28(3): 459-67.

Clarke, S. A., Brooks, R. A., Lee, P. T. and Rushton, N. (2004). The effect of osteogenic growth factors on bone growth into a ceramic filled defect around an implant. *J Orthop Res* 22(5): 1016-24.

Comuzzi, L., Ooms, E. and Jansen, J. A. (2002). Injectable calcium phosphate cement as a filler for bone defects around oral implants: an experimental study in goats. *Clin Oral Implants Res* 13(3): 304-11.

Cook, S. D., Reynolds, M. C., Whitecloud, T. S., Routman, A. S., Harding, A. F., Kay, J. F. and Jarcho, M. (1986). Evaluation of hydroxylapatite graft materials in canine cervical spine fusions. *Spine (Phila Pa 1976)* 11(4): 305-9.

Cool, S., Jackson, R., Pincus, P., Dickinson, I. and Nurcombe, V. (2002). Fibroblast growth factor receptor 4 (FGFR4) expression in newborn murine calvaria and primary osteoblast cultures. *Int J Dev Biol* 46(4): 519-23.

Cowan, C. M., Shi, Y. Y., Aalami, O. O., Chou, Y. F., Mari, C., Thomas, R., Quarto, N., Contag, C. H., Wu, B. and Longaker, M. T. (2004). Adipose-derived adult stromal cells heal critical-size mouse calvarial defects. *Nat Biotechnol* 22(5): 560-7.

Curodeau, A., Sachs, E. and Caldarise, S. (2000). Design and fabrication of cast

orthopedic implants with freeform surface textures from 3-D printed ceramic shell. *J Biomed Mater Res* 53(5): 525-35.

Damien, C. J., Parsons, J. R., Prewett, A. B., Rietveld, D. C. and Zimmerman, M. C. (1994). Investigation of an organic delivery system for demineralized bone matrix in a delayed-healing cranial defect model. *J Biomed Mater Res* 28(5): 553-61.

Delezoide, A. L., Benoist-Lasselien, C., Legeai-Mallet, L., Le Merrer, M., Munnich, A., Vekemans, M. and Bonaventure, J. (1998). Spatio-temporal expression of FGFR 1, 2 and 3 genes during human embryo-fetal ossification. *Mech Dev* 77(1): 19-30.

Denny, H. and SJ, B. (2000). Fracture Complications. A guide to canine and feline orthopaedic surgery. MA, Blackwell Science: 132-151.

Desjardins, R. P. (1985). Hydroxyapatite for alveolar ridge augmentation: indications and problems. *J Prosthet Dent* 54(3): 374-83.

Dhem, A., Piret, N. and Fortunati, D. (1976). Tetracyclines, doxycycline and calcified tissues. *Scand J Infect Dis Suppl*(9): 42-6.

Dong, X., Wang, Q., Wu, T. and Pan, H. (2007). Understanding adsorption-desorption dynamics of BMP-2 on hydroxyapatite (001) surface. *Biophys J* 93(3): 750-9.

- Draenert, G. F., Draenert, K. and Tischer, T. (2009). Dose-dependent osteoinductive effects of bFGF in rabbits. *Growth Factors* 27(6): 419-24.
- Ducheyne, P. (1987). Bioceramics: material characteristics versus in vivo behavior. *J Biomed Mater Res* 21(A2 Suppl): 219-36.
- Einhorn, T. A., Lane, J. M., Burstein, A. H., Kopman, C. R. and Vigorita, V. J. (1984). The healing of segmental bone defects induced by demineralized bone matrix. A radiographic and biomechanical study. *J Bone Joint Surg Am* 66(2): 274-9.
- Elbein, A. D., Pan, Y. T., Pastuszak, I. and Carroll, D. (2003). New insights on trehalose: a multifunctional molecule. *Glycobiology* 13(4): 17R-27R.
- Eppley, B. L., Doucet, M., Connolly, D. T. and Feder, J. (1988). Enhancement of angiogenesis by bFGF in mandibular bone graft healing in the rabbit. *J Oral Maxillofac Surg* 46(5): 391-8.
- Fialkov, J. A., Holy, C. E., Shoichet, M. S. and Davies, J. E. (2003). In vivo bone engineering in a rabbit femur. *J Craniofac Surg* 14(3): 324-32.
- Frankenburg, E. P., Goldstein, S. A., Bauer, T. W., Harris, S. A. and Poser, R. D. (1998). Biomechanical and histological evaluation of a calcium phosphate cement. *J Bone Joint Surg Am* 80(8): 1112-24.

- Frost, H. M. (1958). Preparation of thin undecalcified bone sections by rapid manual method. *Stain Technol* 33(6): 273-7.
- Fukase, Y., Eanes, E. D., Takagi, S., Chow, L. C. and Brown, W. E. (1990). Setting reactions and compressive strengths of calcium phosphate cements. *J Dent Res* 69(12): 1852-6.
- Genant, H. K., Gordon, C., Jiang, Y., Lang, T. F., Link, T. M. and Majumdar, S. (1999). Advanced imaging of bone macro and micro structure. *Bone* 25(1): 149-52.
- Ginebra, M. P., Traykova, T. and Planell, J. A. (2006). Calcium phosphate cements as bone drug delivery systems: a review. *J Control Release* 113(2): 102-10.
- Givol, D. and Yayon, A. (1992). Complexity of FGF receptors: genetic basis for structural diversity and functional specificity. *Faseb J* 6(15): 3362-9.
- Gospodarowicz, D. (1990). Fibroblast growth factor. Chemical structure and biologic function. *Clin Orthop Relat Res*(257): 231-48.
- Goto, T., Kojima, T., Iijima, T., Yokokura, S., Kawano, H., Yamamoto, A. and Matsuda, K. (2001). Resorption of synthetic porous hydroxyapatite and replacement by newly formed bone. *J Orthop Sci* 6(5): 444-7.
- Habraken, W. J., Wolke, J. G. and Jansen, J. A. (2007). Ceramic composites as matrices

and scaffolds for drug delivery in tissue engineering. *Adv Drug Deliv Rev* 59(4-5): 234-48.

Haque, T., Amako, M., Nakada, S., Lauzier, D. and Hamdy, R. C. (2007). An immunohistochemical analysis of the temporal and spatial expression of growth factors FGF 1, 2 and 18, IGF 1 and 2, and TGFbeta1 during distraction osteogenesis. *Histol Histopathol* 22(2): 119-28.

Hauschka, P. V., Mavrakos, A. E., Iafrati, M. D., Doleman, S. E. and Klagsbrun, M. (1986). Growth factors in bone matrix. Isolation of multiple types by affinity chromatography on heparin-Sepharose. *J Biol Chem* 261(27): 12665-74.

Hayashi, K., Kubo, T., Doi, K., Tabata, Y. and Akagawa, Y. (2007). Development of new drug delivery system for implant bone augmentation using a basic fibroblast growth factor-gelatin hydrogel complex. *Dent Mater J* 26(2): 170-7.

Haynesworth, S. E., Goshima, J., Goldberg, V. M. and Caplan, A. I. (1992). Characterization of cells with osteogenic potential from human marrow. *Bone* 13(1): 81-8.

He, L. H., Standard, O. C., Huang, T. T., Latella, B. A. and Swain, M. V. (2008). Mechanical behaviour of porous hydroxyapatite. *Acta Biomater* 4(3): 577-86.

Hollinger, J. O. and Kleinschmidt, J. C. (1990). The critical size defect as an experimental

model to test bone repair materials. *J Craniofac Surg* 1(1): 60-8.

Hollinger, J. O., Brekke, J., Gruskin, E. and Lee, D. (1996). Role of bone substitutes. *Clin Orthop Relat Res*(324): 55-65.

Hollister, S. J., Lin, C. Y., Saito, E., Lin, C. Y., Schek, R. D., Taboas, J. M., Williams, J. M., Partee, B., Flanagan, C. L., Diggs, A., Wilke, E. N., Van Lenthe, G. H., Muller, R., Wirtz, T., Das, S., Feinberg, S. E. and Krebsbach, P. H. (2005). Engineering craniofacial scaffolds. *Orthod Craniofac Res* 8(3): 162-73.

Holmes, R. E., Bucholz, R. W. and Mooney, V. (1987). Porous hydroxyapatite as a bone graft substitute in diaphyseal defects: a histometric study. *J Orthop Res* 5(1): 114-21.

Hosokawa, R., Kikuzaki, K., Kimoto, T., Matsuura, T., Chiba, D., Wadamoto, M., Sato, Y., Maeda, M., Sano, A. and Akagawa, Y. (2000). Controlled local application of basic fibroblast growth factor (FGF-2) accelerates the healing of GBR. An experimental study in beagle dogs. *Clin Oral Implants Res* 11(4): 345-53.

Hutmacher, D. W. and Cool, S. (2007). Concepts of scaffold-based tissue engineering--the rationale to use solid free-form fabrication techniques. *J Cell Mol Med* 11(4): 654-69.

Igawa, K., Mochizuki, M., Sugimori, O., Shimizu, K., Yamazawa, K., Kawaguchi, H.,

Nakamura, K., Takato, T., Nishimura, R., Suzuki, S., Anzai, M., Chung, U. I. and Sasaki, N. (2006). Tailor-made tricalcium phosphate bone implant directly fabricated by a three-dimensional ink-jet printer. *J Artif Organs* 9(4): 234-40.

Ikeuchi, M., Yamamoto, H., Shibata, T. and Otani, M. (2001). Mechanical augmentation of the vertebral body by calcium phosphate cement injection. *Journal of orthopaedic science : official journal of the Japanese Orthopaedic Association* 6(1): 39-45.

Ishikawa, K. and Asaoka, K. (1995). Estimation of ideal mechanical strength and critical porosity of calcium phosphate cement. *J Biomed Mater Res* 29(12): 1537-43.

Ishikawa, K., Takagi, S., Chow, L. and Ishikawa, Y. (1995). Properties and mechanisms of fast-setting calcium phosphate cements. *J Mater Sci Mater Med* 6: 528-533.

Jaiswal, N., Haynesworth, S. E., Caplan, A. I. and Bruder, S. P. (1997). Osteogenic differentiation of purified, culture-expanded human mesenchymal stem cells in vitro. *J Cell Biochem* 64(2): 295-312.

Jarcho, M. (1986). Biomaterial aspects of calcium phosphates. Properties and applications. *Dent Clin North Am* 30(1): 25-47.

Jaye, M., Schlessinger, J. and Dionne, C. A. (1992). Fibroblast growth factor receptor tyrosine kinases: molecular analysis and signal transduction. *Biochim Biophys*

Acta 1135(2): 185-99.

Johnson, K. D., August, A., Sciadini, M. F. and Smith, C. (1996). Evaluation of ground cortical autograft as a bone graft material in a new canine bilateral segmental long bone defect model. *J Orthop Trauma* 10(1): 28-36.

Kamakura, S., Sasano, Y., Homma, H., Suzuki, O., Kagayama, M. and Motegi, K. (2001). Implantation of octacalcium phosphate nucleates isolated bone formation in rat skull defects. *Oral Dis* 7(4): 259-65.

Kato, T., Kawaguchi, H., Hanada, K., Aoyama, I., Hiyama, Y., Nakamura, T., Kuzutani, K., Tamura, M., Kurokawa, T. and Nakamura, K. (1998). Single local injection of recombinant fibroblast growth factor-2 stimulates healing of segmental bone defects in rabbits. *J Orthop Res* 16(6): 654-9.

Kawaguchi, H. (2005). [Stimulation of fracture healing by FGFs]. *Nippon Rinsho* 63 Suppl 10: 509-13.

Kawaguchi, H., Kurokawa, T., Hanada, K., Hiyama, Y., Tamura, M., Ogata, E. and Matsumoto, T. (1994). Stimulation of fracture repair by recombinant human basic fibroblast growth factor in normal and streptozotocin-diabetic rats. *Endocrinology* 135(2): 774-81.

Kawaguchi, H., Nakamura, K., Tabata, Y., Ikada, Y., Aoyama, I., Anzai, J., Nakamura, T.,

- Hiyama, Y. and Tamura, M. (2001). Acceleration of fracture healing in nonhuman primates by fibroblast growth factor-2. *J Clin Endocrinol Metab* 86(2): 875-80.
- Kent, J. N., Zide, M. F., Kay, J. F. and Jarcho, M. (1986). Hydroxylapatite blocks and particles as bone graft substitutes in orthognathic and reconstructive surgery. *J Oral Maxillofac Surg* 44(8): 597-605.
- Komaki, H., Tanaka, T., Chazono, M. and Kikuchi, T. (2006). Repair of segmental bone defects in rabbit tibiae using a complex of beta-tricalcium phosphate, type I collagen, and fibroblast growth factor-2. *Biomaterials* 27(29): 5118-26.
- Komuro, Y. (2003). Use of calcium phosphate cement in craniofacial surgery. *Medical Postgraduates* 41(2): 36-40.
- Koshino, T., Kubota, W. and Morii, T. (1995). Bone formation as a reaction to hydraulic hydroxyapatite thermal decomposition product used as bone cement in rabbits. *Biomaterials* 16(2): 125-8.
- Le Nihouannen, D., Komarova, S. V., Gbureck, U. and Barralet, J. E. (2008). Bioactivity of bone resorptive factor loaded on osteoconductive matrices: stability post-dehydration. *Eur J Pharm Biopharm* 70(3): 813-8.
- Levai, J. P., Bringer, O., Descamps, S. and Boisgard, S. (2003). [Xenograft-related complications after filling valgus open wedge tibial osteotomy defects]. *Rev Chir*

Orthop Reparatrice Appar Mot 89(8): 707-11.

Liao, Y. H., Brown, M. B., Nazir, T., Quader, A. and Martin, G. P. (2002). Effects of sucrose and trehalose on the preservation of the native structure of spray-dried lysozyme. *Pharm Res* 19(12): 1847-53.

Lieberman, J. R., Daluiski, A. and Einhorn, T. A. (2002). The role of growth factors in the repair of bone. *Biology and clinical applications. J Bone Joint Surg Am* 84-A(6): 1032-44.

Lieberman, J. R., Daluiski, A., Stevenson, S., Wu, L., McAllister, P., Lee, Y. P., Kabo, J. M., Finerman, G. A., Berk, A. J. and Witte, O. N. (1999). The effect of regional gene therapy with bone morphogenetic protein-2-producing bone-marrow cells on the repair of segmental femoral defects in rats. *J Bone Joint Surg Am* 81(7): 905-17.

Liu, Y., Hunziker, E. B., Randall, N. X., de Groot, K. and Layrolle, P. (2003). Proteins incorporated into biomimetically prepared calcium phosphate coatings modulate their mechanical strength and dissolution rate. *Biomaterials* 24(1): 65-70.

Liuyun, J., Yubao, L. and Chengdong, X. (2009). Preparation and biological properties of a novel composite scaffold of nano-hydroxyapatite/chitosan/carboxymethyl cellulose for bone tissue engineering. *J Biomed Sci* 16: 65.

- Mankin, H. J., Hornicek, F. J. and Raskin, K. A. (2005). Infection in massive bone allografts. *Clin Orthop Relat Res*(432): 210-6.
- Mansukhani, A., Bellosta, P., Sahni, M. and Basilico, C. (2000). Signaling by fibroblast growth factors (FGF) and fibroblast growth factor receptor 2 (FGFR2)-activating mutations blocks mineralization and induces apoptosis in osteoblasts. *J Cell Biol* 149(6): 1297-308.
- Martin, I., Muraglia, A., Campanile, G., Cancedda, R. and Quarto, R. (1997). Fibroblast growth factor-2 supports ex vivo expansion and maintenance of osteogenic precursors from human bone marrow. *Endocrinology* 138(10): 4456-62.
- Matsumoto, T., Okazaki, M., Inoue, M., Yamaguchi, S., Kusunose, T., Toyonaga, T., Hamada, Y. and Takahashi, J. (2004). Hydroxyapatite particles as a controlled release carrier of protein. *Biomaterials* 25(17): 3807-12.
- Midy, V., Rey, C., Bres, E. and Dard, M. (1998). Basic fibroblast growth factor adsorption and release properties of calcium phosphate. *J Biomed Mater Res* 41(3): 405-11.
- Millis, D. and Jacson, A. (2001). Delayed unions, Nonunions, and Malunions. Textbook of Small Animal Surgery. Philadelphia, SAUNDERS: 1676-1685.
- Minutoli, L., Altavilla, D., Bitto, A., Polito, F., Bellocco, E., Lagana, G., Fiumara, T., Magazu, S., Migliardo, F., Venuti, F. S. and Squadrito, F. (2008). Trehalose: a

biophysics approach to modulate the inflammatory response during endotoxic shock. *Eur J Pharmacol* 589(1-3): 272-80.

Miyamoto, Y., Ishikawa, K., Fukao, H., Sawada, M., Nagayama, M., Kon, M. and Asaoka, K. (1995). In vivo setting behaviour of fast-setting calcium phosphate cement. *Biomaterials* 16(11): 855-60.

Montero, A., Okada, Y., Tomita, M., Ito, M., Tsurukami, H., Nakamura, T., Doetschman, T., Coffin, J. D. and Hurley, M. M. (2000). Disruption of the fibroblast growth factor-2 gene results in decreased bone mass and bone formation. *J Clin Invest* 105(8): 1085-93.

Moore, W. R., Graves, S. E. and Bain, G. I. (2001). Synthetic bone graft substitutes. *ANZ J Surg* 71(6): 354-61.

Murakami, S., Takayama, S., Kitamura, M., Shimabukuro, Y., Yanagi, K., Ikezawa, K., Saho, T., Nozaki, T. and Okada, H. (2003). Recombinant human basic fibroblast growth factor (bFGF) stimulates periodontal regeneration in class II furcation defects created in beagle dogs. *J Periodontal Res* 38(1): 97-103.

Nagai, H., Tsukuda, R. and Mayahara, H. (1995). Effects of basic fibroblast growth factor (bFGF) on bone formation in growing rats. *Bone* 16(3): 367-73.

Nagase, M., Chen, R. B., Asada, Y. and Nakajima, T. (1989). Radiographic and

microscopic evaluation of subperiosteally implanted blocks of hydrated and hardened alpha-tricalcium phosphate in rabbits. *J Oral Maxillofac Surg* 47(6): 582-6.

Nair, M. B., Varma, H., Shenoy, S. J. and John, A. (2009). The treatment of goat femur segmental defects with silica coated hydroxyapatite - one year follow up. *Tissue Eng Part A*. 15 [Electronic article]

Nakadate, M., Amizuka, N., Li, M., Freitas, P. H., Oda, K., Nomura, S., Uoshima, K. and Maeda, T. (2008). Histological evaluation on bone regeneration of dental implant placement sites grafted with a self-setting alpha-tricalcium phosphate cement. *Microsc Res Tech* 71(2): 93-104.

Nakajima, F., Nakajima, A., Ogasawara, A., Moriya, H. and Yamazaki, M. (2007). Effects of a single percutaneous injection of basic fibroblast growth factor on the healing of a closed femoral shaft fracture in the rat. *Calcif Tissue Int* 81(2): 132-8.

Nakamura, T., Hanada, K., Tamura, M., Shibanushi, T., Nigi, H., Tagawa, M., Fukumoto, S. and Matsumoto, T. (1995). Stimulation of endosteal bone formation by systemic injections of recombinant basic fibroblast growth factor in rats. *Endocrinology* 136(3): 1276-84.

Nakamura, T., Hara, Y., Tagawa, M., Tamura, M., Yuge, T., Fukuda, H. and Nigi, H. (1998). Recombinant human basic fibroblast growth factor accelerates fracture

healing by enhancing callus remodeling in experimental dog tibial fracture. *J Bone Miner Res* 13(6): 942-9.

Naski, M. C. and Ornitz, D. M. (1998). FGF signaling in skeletal development. *Front Biosci* 3: d781-94.

Niedhart, C., Maus, U., Miltner, O., Graber, H. G., Niethard, F. U. and Siebert, C. H. (2004). The effect of basic fibroblast growth factor on bone regeneration when released from a novel in situ setting tricalcium phosphate cement. *J Biomed Mater Res A* 69(4): 680-5.

O'Brien, F. J., Taylor, D. and Lee, T. C. (2002). An improved labelling technique for monitoring microcrack growth in compact bone. *J Biomech* 35(4): 523-6.

Oi, Y., Ota, M., Yamamoto, S., Shibukawa, Y. and Yamada, S. (2009). Beta-tricalcium phosphate and basic fibroblast growth factor combination enhances periodontal regeneration in intrabony defects in dogs. *Dent Mater J* 28(2): 162-9.

Okazaki, H., Kurokawa, T., Nakamura, K., Matsushita, T., Mamada, K. and Kawaguchi, H. (1999). Stimulation of bone formation by recombinant fibroblast growth factor-2 in callotaxis bone lengthening of rabbits. *Calcif Tissue Int* 64(6): 542-6.

Oklund, S. A., Prolo, D. J., Gutierrez, R. V. and King, S. E. (1986). Quantitative comparisons of healing in cranial fresh autografts, frozen autografts and

processed autografts, and allografts in canine skull defects. *Clin Orthop Relat Res*(205): 269-91.

Onuma, K., Kanzaki, N. and Kobayashi, N. (2004). Association of calcium phosphate and fibroblast growth factor-2: a dynamic light scattering study. *Macromol Biosci* 4(1): 39-46.

Orr-Urtreger, A., Givol, D., Yayon, A., Yarden, Y. and Lonai, P. (1991). Developmental expression of two murine fibroblast growth factor receptors, flg and bek. *Development* 113(4): 1419-34.

Pautke, C., Tischer, T., Vogt, S., Haczek, C., Deppe, H., Neff, A., Horch, H. H., Schieker, M. and Kolk, A. (2007). New advances in fluorochrome sequential labelling of teeth using seven different fluorochromes and spectral image analysis. *J Anat* 210(1): 117-21.

Pautke, C., Vogt, S., Tischer, T., Wexel, G., Deppe, H., Milz, S., Schieker, M. and Kolk, A. (2005). Polychrome labeling of bone with seven different fluorochromes: enhancing fluorochrome discrimination by spectral image analysis. *Bone* 37(4): 441-5.

Petite, H., Viateau, V., Bensaid, W., Meunier, A., de Pollak, C., Bourguignon, M., Oudina, K., Sedel, L. and Guillemain, G. (2000). Tissue-engineered bone regeneration. *Nat Biotechnol* 18(9): 959-63.

Pinholt, E. M. and Kwon, P. H. (1990). Triple bone labeling of canine mandibles. *Oral Surg Oral Med Oral Pathol* 70(4): 401-5.

Powers, C. J., McLeskey, S. W. and Wellstein, A. (2000). Fibroblast growth factors, their receptors and signaling. *Endocr Relat Cancer* 7(3): 165-97.

Presta, M. and Rifkin, D. B. (1988). New aspects of blood vessel growth: tumor and tissue-derived angiogenesis factors. *Haemostasis* 18(1): 6-17.

Propper, R. H. (1985). A technique for controlled placement of hydroxylapatite over atrophic mandibular ridges. *J Oral Maxillofac Surg* 43(6): 469-70.

Rahn, B. A. and Perren, S. M. (1972). [Alizarin complexon-fluorochrome for bone and dentine labeling]. *Experientia* 28(2): 180.

Ramay, H. R. and Zhang, M. (2004). Biphasic calcium phosphate nanocomposite porous scaffolds for load-bearing bone tissue engineering. *Biomaterials* 25(21): 5171-80.

Ratner, B. D. and Bryant, S. J. (2004). Biomaterials: where we have been and where we are going. *Annu Rev Biomed Eng* 6: 41-75.

Richards, A. B., Krakowka, S., Dexter, L. B., Schmid, H., Wolterbeek, A. P., Waalkens-Berendsen, D. H., Shigoyuki, A. and Kurimoto, M. (2002). Trehalose: a review of

properties, history of use and human tolerance, and results of multiple safety studies. *Food Chem Toxicol* 40(7): 871-98.

Rifkin, D. B. and Moscatelli, D. (1989). Recent developments in the cell biology of basic fibroblast growth factor. *J Cell Biol* 109(1): 1-6.

Rodan, S. B., Wesolowski, G., Thomas, K. A., Yoon, K. and Rodan, G. A. (1989). Effects of acidic and basic fibroblast growth factors on osteoblastic cells. *Connect Tissue Res* 20(1-4): 283-8.

Schmitz, J. P. and Hollinger, J. O. (1986). The critical size defect as an experimental model for craniomandibulofacial nonunions. *Clin Orthop Relat Res*(205): 299-308.

Schram, W. R. and Fosdick, L. S. (1948). Stimulation of healing in long bones by use of artificial material. *J Oral Surg (Chic)* 6(3): 209-17.

Segal, U. and Shani, J. (2009). Surgical management of large segmental femoral and radial bone defects in a dog. *Vet Comp Orthop Traumatol* 23(1).

Sen, M. K. and Miclau, T. (2007). Autologous iliac crest bone graft: should it still be the gold standard for treating nonunions? *Injury* 38 Suppl 1: S75-80.

Seshima, H., Yoshinari, M., Takemoto, S., Hattori, M., Kawada, E., Inoue, T. and Oda, Y.

- (2006). Control of bisphosphonate release using hydroxyapatite granules. *J Biomed Mater Res B Appl Biomater* 78(2): 215-21.
- Shapiro, F. (2008). Bone development and its relation to fracture repair. The role of mesenchymal osteoblasts and surface osteoblasts. *Eur Cell Mater* 15: 53-76.
- Simpson, D. and Keating, J. F. (2004). Outcome of tibial plateau fractures managed with calcium phosphate cement. *Injury* 35(9): 913-8.
- Stevenson, S. (1999). Biology of bone grafts. *Orthop Clin North Am* 30(4): 543-52.
- Stevenson, S., Shaffer, J. W. and Goldberg, V. M. (1996). The humoral response to vascular and nonvascular allografts of bone. *Clin Orthop Relat Res*(326): 86-95.
- Suda, T. (2007). The cells of hard tissues and its differentiation. Bon Biology. Tokyo, Ishiyaku publishers: 75-126.
- Suda, T (2007). Mechanism of calcification. Bone biology. Tokyo, Ishiyaku publishers: 145-174.
- Suda., T. (2007). Remodelling and modelling in the bone. Bone biology. Tokyo, Ishiyaku publishers: 231-247.
- Sullivan, R. and Klagsbrun, M. (1985). Purification of cartilage-derived growth factor by

heparin affinity chromatography. *J Biol Chem* 260(4): 2399-403.

Sum, A. K., Faller, R. and de Pablo, J. J. (2003). Molecular simulation study of phospholipid bilayers and insights of the interactions with disaccharides. *Biophys J* 85(5): 2830-44.

Sun, W., Darling, A., Starly, B. and Nam, J. (2004). Computer-aided tissue engineering: overview, scope and challenges. *Biotechnol Appl Biochem* 39(Pt 1): 29-47.

Suzuki, H. K. and Mathews, A. (1966). Two-color fluorescent labeling of mineralizing tissues with tetracycline and 2,4-bis[N,N'-di-(carbomethyl)aminomethyl] fluorescein. *Stain Technol* 41(1): 57-60.

Sweeney, T. M., Opperman, L. A., Persing, J. A. and Ogle, R. C. (1995). Repair of critical size rat calvarial defects using extracellular matrix protein gels. *J Neurosurg* 83(4): 710-5.

Tabata, Y., Yamada, K., Miyamoto, S., Nagata, I., Kikuchi, H., Aoyama, I., Tamura, M. and Ikada, Y. (1998). Bone regeneration by basic fibroblast growth factor complexed with biodegradable hydrogels. *Biomaterials* 19(7-9): 807-15.

Takemasa, R. and Yamamoto, H. (2002). [Bioactive calcium phosphate paste injection for repair of vertebral fracture due to osteoporosis]. *Nippon Rinsho* 60 Suppl 3: 696-703.

- Talal, A., Waheed, N., Al-Masri, M., McKay, I. J., Tanner, K. E. and Hughes, F. J. (2009). Absorption and release of protein from hydroxyapatite-poly(lactic acid) (HA-PLA) membranes. *J Dent* 37(11): 820-6.
- Tanag, M. A., Madura, T., Yano, K. and Hosokawa, K. (2006). Use of calcium phosphate cement paste in orbital volume augmentation. *Plast Reconstr Surg* 117(4): 1186-93.
- Tazaki, J., Murata, M., Akazawa, T., Yamamoto, M., Ito, K., Arisue, M., Shibata, T. and Tabata, Y. (2009). BMP-2 release and dose-response studies in hydroxyapatite and beta-tricalcium phosphate. *Biomed Mater Eng* 19(2-3): 141-6.
- Thomas, K. A. (1987). Fibroblast growth factors. *Faseb J* 1(6): 434-40.
- Thoren, K. and Aspenberg, P. (1993). Effects of basic fibroblast growth factor on bone allografts. A study using bone harvest chambers in rabbits. *Ann Chir Gynaecol Suppl* 207: 129-35.
- Trombelli, L., Heitz-Mayfield, L. J., Needleman, I., Moles, D. and Scabbia, A. (2002). A systematic review of graft materials and biological agents for periodontal intraosseous defects. *J Clin Periodontol* 29 Suppl 3: 117-35; discussion 160-2.
- Twal, W. O., Vasilatos-Younken, R., Gay, C. V. and Leach, R. M., Jr. (1994). Isolation and

localization of basic fibroblast growth factor-immunoreactive substance in the epiphyseal growth plate. *J Bone Miner Res* 9(11): 1737-44.

van Gaalen, S., Kruyt, M., Geuze, R., de Bruijn, J., Alblas, J. and Dhert, W. (2009). The use of fluorochrome labels for in vivo bone tissue engineering research. *Tissue Eng Part B Rev*.

Villanueva, A. R. (1974). A bone stain for osteoid seams in fresh, unembedded, mineralized bone. *Stain Technol* 49(1): 1-8.

Villanueva, A. R. and Lundin, K. D. (1989). A versatile new mineralized bone stain for simultaneous assessment of tetracycline and osteoid seams. *Stain Technol* 64(3): 129-38.

Wang, J. S. and Aspenberg, P. (1996). Basic fibroblast growth factor enhances bone-graft incorporation: dose and time dependence in rats. *J Orthop Res* 14(2): 316-23.

Wang, J. S. and Aspenberg, P. (1996). Basic fibroblast growth factor promotes bone ingrowth in porous hydroxyapatite. *Clin Orthop Relat Res*(333): 252-60.

Wassell, D. T., Hall, R. C. and Embery, G. (1995). Adsorption of bovine serum albumin onto hydroxyapatite. *Biomaterials* 16(9): 697-702.

Webb, P. A. (2000). A review of rapid prototyping (RP) techniques in the medical and

biomedical sector. *J Med Eng Technol* 24(4): 149-53.

Wildburger, R., Zarkovic, N., Egger, G., Petek, W., Zarkovic, K. and Hofer, H. P. (1994).

Basic fibroblast growth factor (BFGF) immunoreactivity as a possible link between head injury and impaired bone fracture healing. *Bone Miner* 27(3): 183-92.

Willart, J. F., Hedoux, A., Guinet, Y., Danede, F., Paccou, L., Capet, F. and Descamps, M.

(2006). Metastability release of the form alpha of trehalose by isothermal solid state vitrification. *J Phys Chem B* 110(23): 11040-3.

Wronski, T. J. (2001). Skeletal effects of systemic treatment with basic fibroblast growth

factor. *J Musculoskelet Neuronal Interact* 2(1): 9-14.

Xu, X. L., Tang, T., Dai, K., Zhu, Z., Guo, X. E., Yu, C. and Lou, J. (2005). Immune

response and effect of adenovirus-mediated human BMP-2 gene transfer on the repair of segmental tibial bone defects in goats. *Acta Orthop* 76(5): 637-46.

Yamaguchi, A., Komori, T. and Suda, T. (2000). Regulation of osteoblast differentiation

mediated by bone morphogenetic proteins, hedgehogs, and Cbfa1. *Endocr Rev* 21(4): 393-411.

Yaszemski, M. J., Payne, R. G., Hayes, W. C., Langer, R. and Mikos, A. G. (1996).

Evolution of bone transplantation: molecular, cellular and tissue strategies to

engineer human bone. *Biomaterials* 17(2): 175-85.

Ziegler, J., Mayr-Wohlfart, U., Kessler, S., Breitig, D. and Gunther, K. P. (2002).

Adsorption and release properties of growth factors from biodegradable implants.

*J Biomed Mater Res* 59(3): 422-8.